ornl

ORNL/TM-9085

OAK RIDGE NATIONAL LABORATORY

MARTIN MARIETTA

Irradiation Performance of HTGR Coated Particle Fuels With ZrC Coatings

F. J. Homan
M. J. Kania

[redacted]

OPERATED BY
MARTIN MARIETTA ENERGY SYSTEMS, INC.
FOR THE UNITED STATES
DEPARTMENT OF ENERGY

Printed in the United States of America. Available from
the U.S. Department of Energy
Technical Information Center
P.O. Box 62, Oak Ridge, Tennessee 37830

ORNL/TM-9085
Distribution
Category UC-77

METALS AND CERAMICS DIVISION

Fueled Graphite Development
(FTP/A HTR0100, WBS 1601.02)

IRRADIATION PERFORMANCE OF HTGR COATED PARTICLE FUELS WITH ZrC COATINGS

F. J. Homan and M. J. Kania

NOTICE: This document contains information of a preliminary nature. It is subject to revision or correction and therefore does not represent a final report.

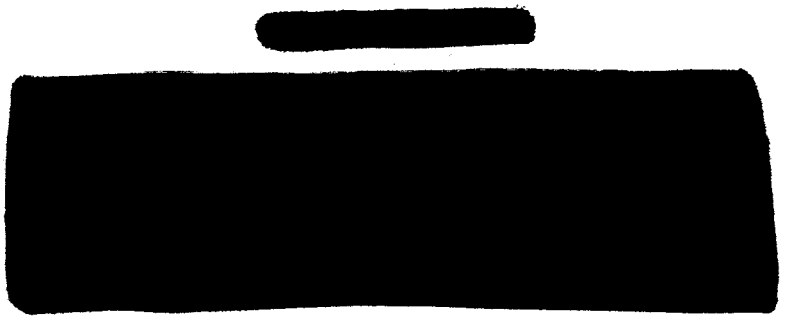

Date Published: January 1985

Prepared for
Office of Converter Reactor Deployment

Prepared by the
OAK RIDGE NATIONAL LABORATORY
Oak Ridge, Tennessee 37831
operated by
MARTIN MARIETTA ENERGY SYSTEMS, INC.
for the
U.S. DEPARTMENT OF ENERGY
under Contract No. DE-AC05-840R21400

CONTENTS

IRRADIATION PERFORMANCE OF HTGR COATED PARTICLE FUELS WITH ZrC COATINGS*

F. J. Homan and M. J. Kania

ABSTRACT

During the past 25 years of fuel development for the High-Temperature Gas-Cooled Reactor (HTGR) the Triso particle has evolved as the favored design to optimize economics and performance. The Triso particle consists of a kernel (fissile or fertile), a buffer [porous pyrocarbon (PyC)], an inner PyC layer, a dense SiC layer, and an outer PyC layer. The SiC layer is the primary barrier to the release of both metallic and gaseous fission products from the particle. Consideration has been given to replacing the SiC layer with ZrC for applications requiring very high fuel operating temperatures. Zirconium carbide is more refractory than silicon carbide (3540°C melting temperature compared with 2700°C for SiC) and denser (6.73 g/cm^3 compared with 2.217 for SiC) and therefore has the potential for being a better fission product barrier. Other designs using ZrC have also been considered and tested. The testing done to date on HTGR fuel particles with ZrC coatings has been very limited compared with the testing done on the Triso particle design. Most of the data have been collected on isolated specimens included in experiments planned to test reference designs. This report reviews all the irradiation testing data collected within the U.S. program on HTGR fuel particles with ZrC coatings. Fission product retentiveness of particles with ZrC coatings has generally been inferior to that of similar particles with the Triso design, but it is emphasized that the fabrication of ZrC coatings has not been optimized to nearly the extent of that of SiC coatings.

*Research sponsored by Office of Converter Reactor Deployment, Division of HTR Development, U.S. Department of Energy, under contract DE-AC05-840R21400 with Martin Marietta Energy Systems, Inc.

INTRODUCTION

Several different types of High-Temperature Gas-Cooled Reactor (HTGR) fuel particles with ZrC coatings have been fabricated and tested. The "ZrC-Triso" design includes a ZrC coating in place of the SiC in a standard Triso configuration. Some of the early experiments[1] included "Triso 0"* and "Triso I"† particles. "Graded"‡ coating designs have also been tested. Coatings of ZrC were initially thought to offer several advantages over SiC coatings. Because ZrC is more refractory (3540°C melting temperature compared with 2700°C for SiC), particles containing ZrC coatings can withstand higher graphitization temperatures during fuel rod manufacture. Higher graphitization temperatures result in fuel rods with higher thermal conductivity, which, in turn, results in lower irradiation temperatures during reactor operation. In addition, ZrC forms no low-melting compounds with fuel or fission product species. It was therefore thought to be less susceptible to chemical interaction with the fuel than SiC. Also, ZrC coatings have favorable neutronics (relatively few parasitic captures of neutrons), although not quite as favorable as SiC.

Fabrication experience with ZrC coatings is somewhat limited compared with SiC,[1-6] and irradiation data is much less extensive (Table 1). The available irradiation data suggest that, in terms of the most important performance parameter (fission product retention), ZrC coatings do not perform as well as even the worst SiC coatings made with current technology. The ZrC coatings seem to be dimensionally stable and to resist neutron damage, and they are chemically inert compared with SiC. But, in irradiation experiments where fission product retention can be measured,

---

*The Triso 0 design is a kernel, a dense "flash" coating of pyrolytic carbon (PyC), the ZrC coating, a porous carbon (buffer) coating, and a dense PyC coating.

†The Triso I design is a kernel, a buffer layer, a flash seal coating, the ZrC, and then dense PyC.

‡The graded coating design consists of a kernel, buffer, and then dense PyC with gradually increasing ZrC content until pure ZrC is being deposited. In the "double-graded" coating, the graded coating is followed by gradually decreasing ZrC until pure dense PyC is being deposited.

Table 1. Summary of irradiation data on ZrC coatings on HTGR fuel particles

Capsule	Specimen	Dates	Coating type[a]	Kernel type	Specimen	Burnup (% FIMA) ^{235}U	Burnup (% FIMA) ^{238}U	Fluence (neutrons/m^2) $E>29$ fJ	Temperature (°C)	Fabricator[b]
Siloé reactor			Triso 0	UC_2	~100 loose particles	70		5×10^{25}	1200	GA
				$(8Th,U)O_2$	~100 loose particles	8		5	1200	
			Triso 1	UC_2	~100 loose particles	70		5	1200	
				$(8Th,U)O_2$	~100 loose particles	8		5	1200	
HF-28	ES1	Feb–Apr 75		Inert	Loose particles			4	900	LANL
	1A	2136 h		Inert	in end plugs			4	900	
	MS1			Inert				7	1250	
	MS2			Inert				8	1250	
	ES2			Inert				4	900	
HF-29	ES1	Feb–Mar 75		Inert	Loose particles			5	900	LANL
	1A	2675 h		Inert	Extruded graphite wafer			5	900	
	EL1			Inert	Loose particles			10	900	
	1AA			Inert	Extruded graphite wafer			10	900	
	ML1			Inert	Loose particles			11	900	
	ML2			Inert	Loose particles			11	900	
	39A			Inert	Loose particles			10	900	
	MS2			Inert	Loose particles			10	900	
	EL2			Inert	Loose particles			10	900	
	S2A			Inert	Extruded graphite wafer			5	900	
	ES2			Inert	Loose particles			5	900	
HT-31	LANL-1	Mar–Jun 76	Triso-ZrC	Carbon (inert)	Extruded fuel rods			8.65	1250	LANL[c]
	LANL-2	2147 h		Carbon (inert)	W1 UC_2 Triso			8.89	1250	LANL[c]
	LANL-3			Carbon (inert)	ThO_2 Biso and ZrC Triso (on inert kernels)			9.00	1250	LANL[c]
HT-32	LANL-1	Nov–Feb 77	Triso-ZrC	ThO_2	Extruded fuel rods	9.0		9.31	1300	LANL
	LANL-2	2308 h		ThO_2	Extruded fuel rods	9.4		9.56	1300	LANL
	LANL-3			ThO_2	Extruded fuel rods	9.7		9.68	1300	LANL
HRB-7	17	Jan–Jul 74 4405 h	Triso-ZrC	UC_2	Slug injected fuel rod	84.2		4.50	1300	GA
HRB-8	17	Mar–Oct 74 5476 h	Triso-ZrC	UC_2	Slug injected fuel rod	84.4		5.92	1200	GA

Table 1. (continued)

Capsule	Specimen	Dates	Coating type[a]	Kernel type	Specimen	Burnup (% FIMA) ^{235}U	Burnup (% FIMA) ^{238}U	Fluence (neutrons/m^2) $E>29$ fJ	Temperature (°C)	Fabricator[b]
OF-2	A-4-12	Jun 75—	Graded	UC_2	Fuel rod	73.0		5.58	1150	LANL
	B-4-12	Aug 76	ZrC		Fuel rod	79.5		8.36	1350	LANL
	B-4-12 (Spine)	8440 h	Triso		Loose particles	79.5		8.36	1350	LANL
HRB-12	1	Feb 76—	ZrC Triso	WAR $UC_{4.60}O_{1.10}$	Fuel rod	84		4.40	1150	*d*
	2	Jan 77	ZrC, ZrC—doped oPyC	WAR $UC_{4.60}O_{1.10}$	Fuel rod	85		4.94	1200	*d*
	3	6602 h	ZrC, ZrC—doped oPyc, graded ZrC-C	WAR $UC_{4.60}O_{1.10}$	Fuel rod	85		5.40	1200	*d*
	7		ZrC-Triso	WAR $UC_{4.60}O_{1.10}$	Fuel rod	86		6.90	1300	*d*
	8		ZrC, ZrC—doped oPyC	WAR $UC_{4.60}O_{1.10}$	Fuel rod	87		7.14	1300	*d*
	9		ZrC, ZrC—doped oPyC, graded ZrC-C	WAR $UC_{4.60}O_{1.10}$	Fuel rod	87		7.36	1300	*d*
HRB-15a	Rod 2	Jul 80—	Triso	UO_2^{*e}	Fuel rod	81	7.7	4.6	1103	GA
	Rod 3	Jan 81	Triso	UO_2^{*f}	Fuel rod	82	9.3	5.2	1127	GA
	Rod 6	4172 h	ZrC Triso	UO_2	Fuel rod	84	13.3	6.4	1142	GA
	Rod 7		ZrC Triso	UC_2	Fuel rod	84	14.3	6.6	1191	GA
	Rod 9		Triso	UO_2^{*e}	Fuel rod	85	15.4	6.9	1185	GA
	Rod 12		Triso	UO_2^{e}	Fuel rod	85	14.9	6.5	1174	GA
	Monolayer 2		Triso	UO_2^{e}	Bonded monolayer	82	9.3	4.6	1103	GA
	Monolayer 3		Triso	UO_2^{f}	Bonded monolayer	83	10.8	5.2	1127	GA
	Monolayer 9		Triso	UO_2^{e}	Bonded monolayer	85	15.4	6.9	1185	GA
	Monolayer 12		Triso	UO_2^{e}	Bonded monolayer	85	14.9	6.5	1174	GA
	Monolayer 13		ZrC Triso	UC_2	Bonded monolayer	84	14.0	6.2	1147	GA

Table 1. (continued)

Capsule	Specimen	Dates	Coating type[a]	Kernel type	Specimen	Burnup (% FIMA) ^{235}U	Burnup (% FIMA) ^{238}U	Fluence (neutrons/m^2) E>29 fJ	Temperature (°C)	Fabricator[b]
	Tray 2		Triso	UO_2[e]	Loose particle tray	81	7.7	4.6	1103	GA
	Tray 5		ZrC Triso	UC_2	Loose particle tray	84	12.2	6.0	1203	GA
	Tray 6		ZrC Triso	UO_2	Loose particle tray	84	13.3	5.3	1142	GA
	Tray 12		Triso	UO_2[e]	Loose particle tray	85	14.9	6.5	1174	GA
	Tray 15		ZrC Triso	UC_2	Loose particle tray	84	11.5	5.4	1099	GA

[a] oPyC = outer pyrocarbon.

[b] GA = GA Technologies, LANL = Los Alamos National Laboratory.

[c] ZrC-Triso.

[d] ORNL (up to ZrC) and LANL (ZrC outward).

[e] UO_2 kernel followed by dense PyC flash coating, then a thin ZrC coating.

[f] UO_2 kernel followed by buffer layer with ZrC dispersed in it.

either directly or indirectly, they did not retain fission products as well as did the fissile particles with SiC coatings irradiated in the same capsules. Brief summaries of the irradiation experiments conducted on ZrC coatings are given below.

RESULTS OF IRRADIATION TESTING

SILOÉ REACTOR[1]

The UC_2 Triso 0 particles were the only design for which failures were observed during postirradiation stereoscopic examination. Virtually all the zirconium carbide coatings applied directly over the kernels had several radial cracks, and in many instances the cracks propagated through the porous PyC coating but did not penetrate the dense outer PyC (oPyC). Cracking of the ZrC in this particle design was not unexpected because there was no void space inside the ZrC coating to accommodate fission gas pressure. There were no indications of a reaction between the kernel or fission products and the ZrC. The only fission product detected outside the ZrC layer (with the electron microprobe) was cesium.

The UC_2 Triso I particles performed well, with no broken coatings observed during the postirradiation examination. The ZrC coatings were crack free. Significant shrinkage of the porous PyC buffer layer resulted in a considerable gap between this coating and the ZrC. There was no evidence of chemical attack of the ZrC layer by fission products. Electron microprobe examination revealed no cesium outside the ZrC. This suggests that the cesium that escaped through the ZrC in the Triso 0 design migrated through cracks rather than diffused through ZrC.

The $(8Th,U)O_2$ Triso 0 particles had radial cracks similar to those described above for the UC_2 Triso 0 particles. Some of the particles were crack free, probably because of the lower burnup in these particles than in the UC_2 particles (lower fission gas pressures). No broken oPyC coatings were observed, and no chemical attack of the ZrC could be detected with the electron microprobe.

The $(8Th,U)O_2$ Triso I particles performed well. No cracks in the ZrC coatings were observed, and no chemical attack of the ZrC was seen during metallographic examination. Shrinkage of the buffer layer and seal coat left a gap between these layers and the ZrC.

CAPSULES HT-28 AND -29 (ref. 7)

Particles fabricated from inert carbon kernels, a buffer layer, inner PyC (iPyC), and ZrC as the outer layer (no oPyC layer) were undamaged by the irradiation. There appeared to be some evidence of chemical attack of the ZrC outer layer. Close examination of archive particles showed damage also, but to a lesser extent. The chemical attack is thought to be oxidation of the unprotected ZrC.

Particles fabricated from inert carbon kernels with a standard Triso coating design (with ZrC replacing SiC) were undamaged by the irradiation.

Particles fabricated with inert carbon kernels, buffer layers, and graded ZrC-C coatings survived the irradiation, but a few of the particles had small radial cracks through the outermost ZrC layer. The graded ZrC-C coating started out as pure PyC; then ZrC was added, with the ZrC content increasing until the outermost layer was pure ZrC. The cracking may have been due to differences in the irradiation stability of PyC and ZrC.

Particles fabricated with inert carbon kernels, buffer layers, and "double-graded ZrC-C" coatings were irradiated at nominal temperatures of 900°C (in capsule HT-29) and 1250°C (in capsule HT-28). This is also the case for the "single-graded" coatings discussed earlier. Particles with double-graded coatings survived irradiation at 900°C nominal temperature to exposures to 9×10^{25} neutrons/m^2 ($E > 29$ fJ). At exposures up to about 11×10^{25} neutrons/m^2, about 5% of the coatings failed. Examination of these particles with polarized light revealed preferred orientation (anisotropy) within the PyC-rich regions of the graded coating (as was the case with the single-graded coatings). This suggests that failure was due to swelling of the PyC-rich regions of the graded coating while the ZrC regions remained dimensionally stable. Particles irradiated at 1250°C to exposures of about 7.5×10^{25} neutrons/m^2 showed 80% coating failure. About 70% of the particles had lost the outermost graded coating, and about 10% had ruptured ZrC coatings as well as broken outer coatings.

CAPSULE HT-31 (refs. 8, 9)

Three fuel rods were fabricated at Los Alamos National Laboratory (LANL) by its extrusion process. The rods contained Triso-coated UC_2 fissile particles (with 6.36%-enriched uranium), Biso-coated ThO_2 fertile particles, and inert particles with a ZrC-Triso coating design. The extruded rods were irradiated to a fast fluence ($E > 29$ fJ) of about 9.0×10^{25} neutrons/m^2 at about 1250°C. Burnups in the fissile and fertile particles were about 85% FIMA* for the ^{235}U, 18% FIMA for the ^{238}U, and 9% FIMA for the ^{232}Th.

The ZrC coatings on the inert particles performed well. Some cracking was noted in the ZrC layer, but the cracking has been attributed to the stresses that occur during the mounting and polishing process. No coating-matrix interaction was noted, which was attributed to the high-density extruded graphite matrix.

CAPSULE HT-32

Three fuel rods fabricated by LANL were irradiated in capsule HT-32. The rods were fabricated with ZrC-Triso-coated fertile kernels by the LANL extrusion process. It was planned that the rods be returned to LANL for postirradiation examination, but the LANL program was cancelled before the completion of the irradiation. The rods were therefore only given a cursory examination[10] and no details on particle or coating performance are available.

CAPSULES HRB-7 AND -8

Figure 1 shows metallographic displays of particles irradiated in the two capsules. The particle from capsule HRB-7 operated at somewhat higher temperatures, and there is evidence of corrosion of the ZrC layer on the cold side of the particle. The electron microprobe display (Fig. 2) shows that uranium is present in the area where the ZrC coating was attacked. The kernels of these particles contained appreciable amounts of chlorine in the as-fabricated condition presumably due to permeable inner pyrocarbon coatings and the ZrC coating process.[6] Evidently, during irradiation

*Fissions per initial heavy metal atom.

R-65348

(a)

R-66402

(b)

Fig. 1. Triso-coated UC_2 particles. (*a*) Particle from rod 17 of HRB-7 operated at an average temperature of 1360°C and an average temperature gradient of 420°C/cm with the hot side of the particle on the top. (*b*) Particle from rod 17 of HRB-8 operated at an average temperature of 1225°C and an average temperature gradient of 590°C/cm with the hot side of the particle on the top. This coating design employed ZrC instead of SiC and a thin seal coat rather than the reference inner low-temperature isotropic carbon coating.

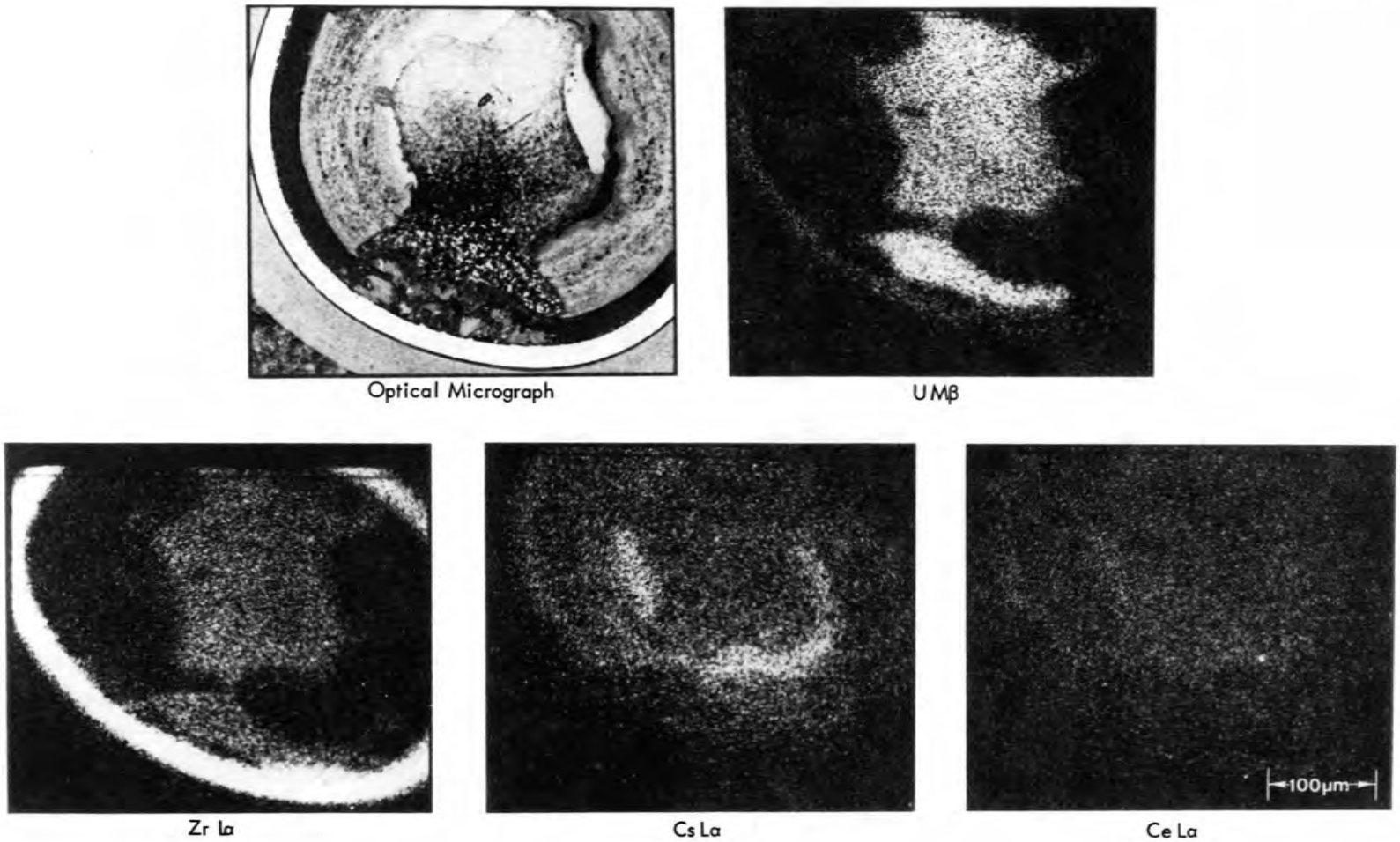

Fig. 2. Distribution of Zr, U, Ce, and Cs in a Triso-coated dense UC_2 particle irradiated in rod 17 of HRB-7 at an average temperature of 1360°C and an average temperature gradient of 420°C/cm. The hot side of the particle is on the bottom. Note the good appearance of the ZrC coating and the high concentration of fission products outside the kernel.

highly volatile uranium chlorides were formed, leading to uranium migration to the ZrC coatings and eventual attack of the ZrC. Although the attack was extensive, the ZrC coating apparently remained intact, as evidenced by the cesium display (Fig. 2). There was no extensive loss of cesium in the region of the attack.

The high concentrations of chlorine in the ZrC coatings is thought to have produced chemically induced porosity in the coatings, as shown at higher magnification (Fig. 3). Chlorine is present in the coating gases used for both SiC and ZrC deposition. No simple quantitative techniques are available to determine precisely the chlorine content in the coating or in the particle after fabrication. Chlorine present in relatively high concentrations has been observed qualitatively during postirradiation electron microprobe examinations in some fuel particles.

Indications of fission product loss from the ZrC-Triso particles come from both the gamma scans of the graphite sleeve and from the microprobe displays (Figs. 2, 4–6). The gamma scans were taken in the energy range 550 to 750 keV, which includes the fission products ^{134}Cs, ^{144}Ce, ^{154}Eu, and ^{95}Zr. The HRB-7 graphite sleeve scan shows fairly high peaks for several of the fuel rod positions. The high peaks are usually associated with rods containing Biso fissile particles. Of particular note here is the high peak associated with rod 17, which contained the ZrC-Triso fissile fuel. The scan for the HRB-8 graphite sleeve does not show this high peak next to rod 17, but this capsule was operated at somewhat lower temperatures. The electron microprobe display (Fig. 4) for the HRB-8 particle studied shows appreciable quantities of both cesium and cerium outside the ZrC coating.

CAPSULE OF-2

Two fuel rods and about 2 cm^3 of loose particles with ZrC coatings were irradiated in capsule OF-2. The fuel rods contained standard Triso-coated UC_2 particles and standard Biso-coated ThO_2 particles along with graded-ZrC-Triso-coated UC_2 particles. The standard Triso- and Biso-coated particles were fabricated by GA Technologies, while the ZrC-coated particles were fabricated by LANL. Graded C-ZrC-C coatings were used on the LANL particles to facilitate postirradiation identification of these

R-65353

R-65354

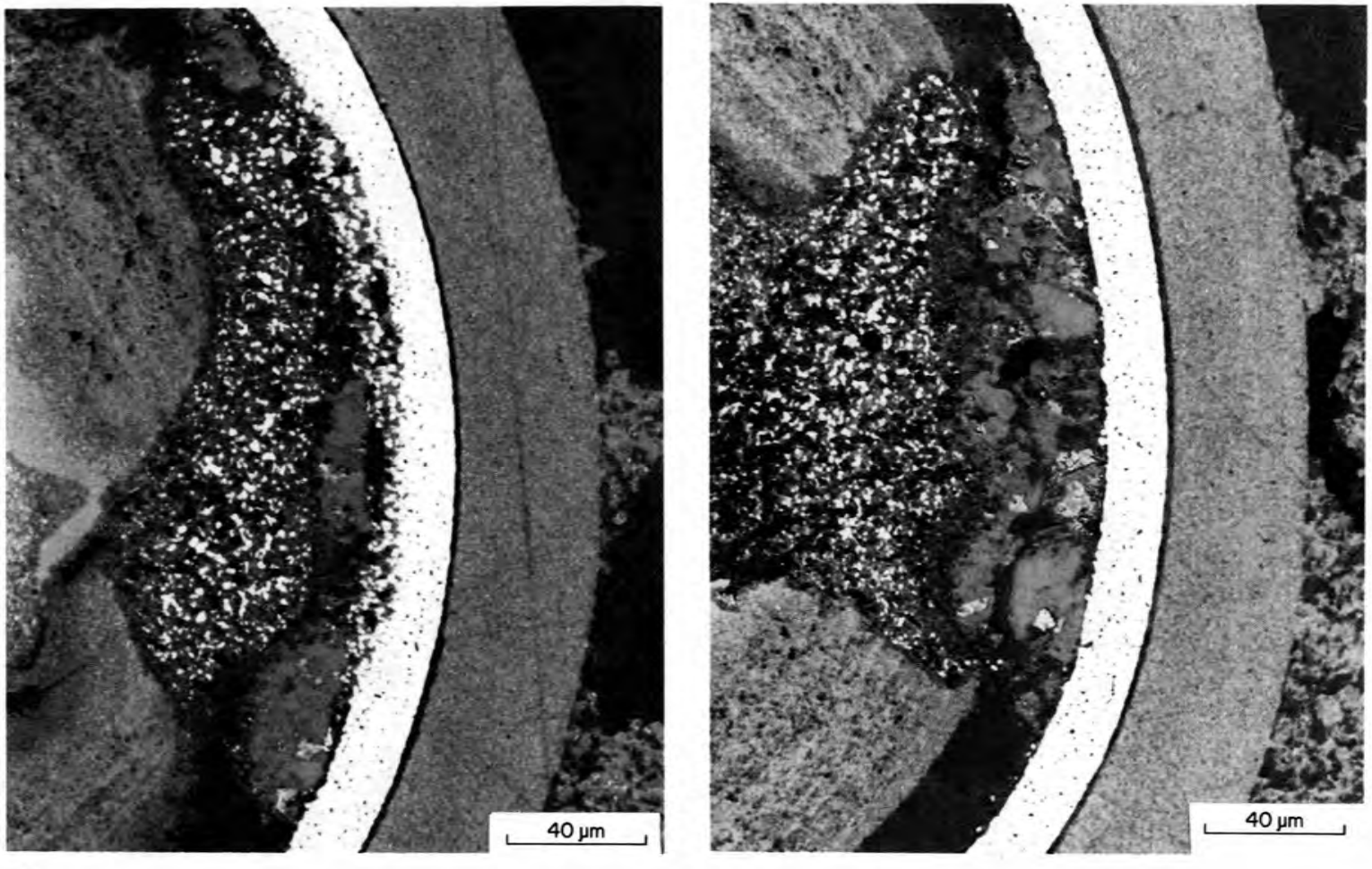

(*a*) (*b*)

Fig. 3. High magnification of ZrC coating from Fig. 1(*a*) showing (*a*) cold side of the particle and (*b*) hot side. The "peppery" appearance of ZrC is thought to be a chemically induced porosity due to residual chlorine for the coating run.

R-72430

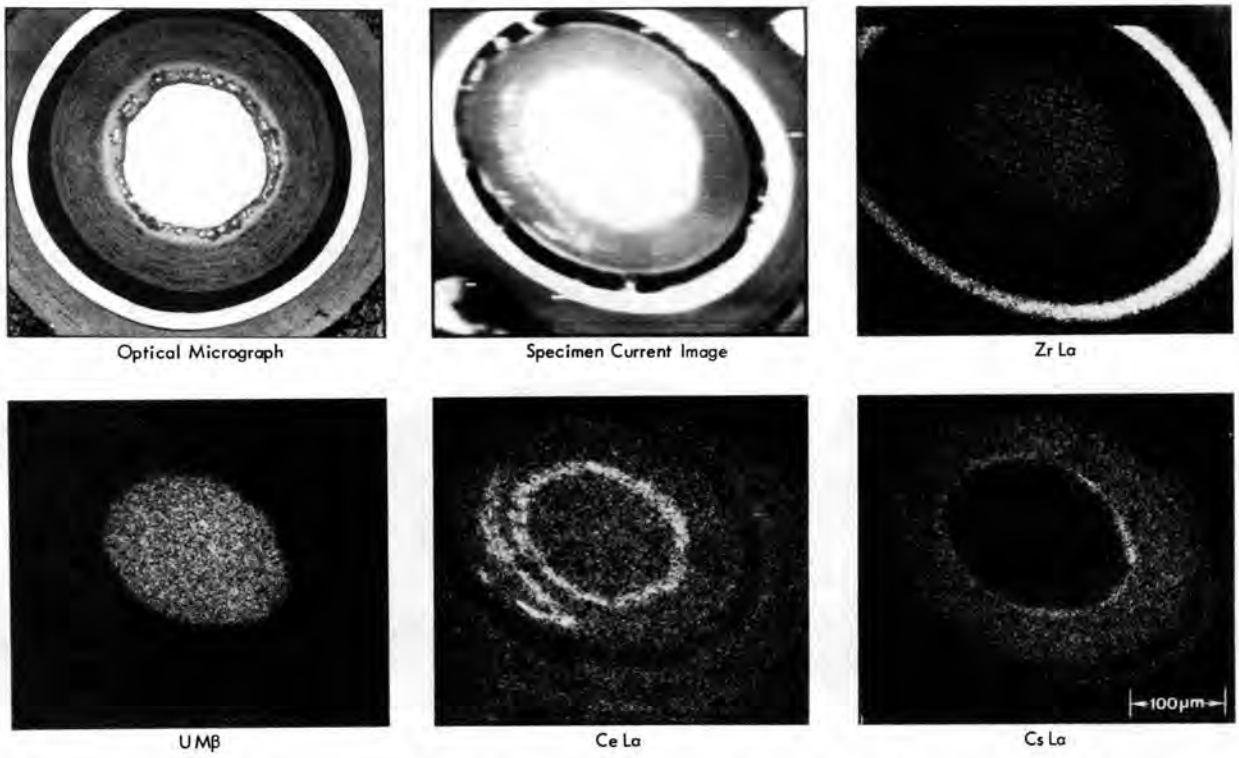

Fig. 4. Distribution of U, Zr, Cs, and Ce in a Triso-coated dense UC_2 particle irradiated in rod 17 of HRB-8 at an average temperature of 1225°C and an average temperature gradient of 590°C/cm. The hot side of the particle is on the top. Note the good appearance of ZrC and the high concentration of rare earth fission products outside the kernel.

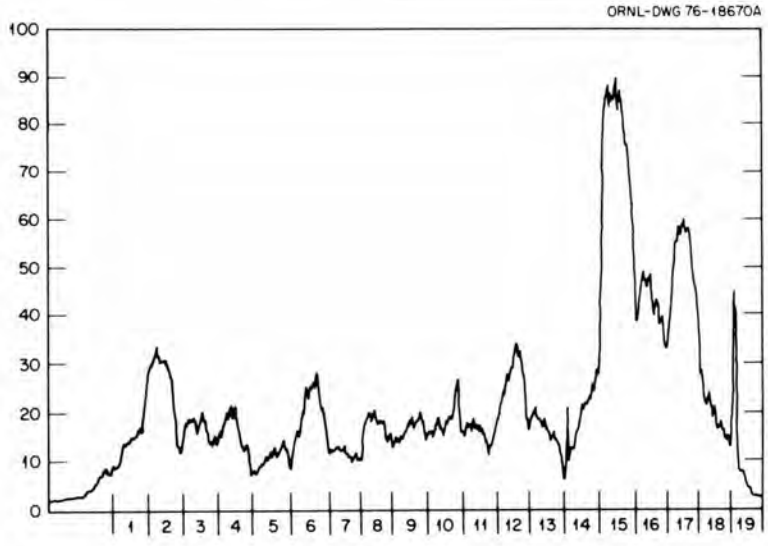

Fig. 5. Gamma scan made along the empty graphite sleeve from HRB-7. The scan was made to include energy peaks in the range 550 to 750 keV, which includes the fission products ^{134}Cs, ^{144}Ce, ^{154}Eu, and ^{95}Zr.

This Page Blank

This Page Blank

Table 2. Visual examination summary for HRB-12 fuel rods

Rod	Fissile Fuel Type[a]	Observations at fuel rod surfaces			
		Debonding	Number of failures		Other
			Outer LTI	SiC or ZrC	
1	WAR, 45, A, ZrC, 43	None	7	7	
2	WAR, 45, A, ZrC, 43	Bottom edge	13	13	
3	WAR, 45, A, ZrC, 43	Bottom edge	6	6	
4	WAR, 44, A, SiC, 48	Top edge	0	0	Re foil and BeO insulator attached
5	WAR, 45, A, SiC, 43	Bottom edge	0	1	1 sooty particle
6	WAR, 44, A, Biso, 50	None	0		100 sooty particles
7	WAR, 45, A, ZrC, 43	Top edge	13	13	
8	WAR, 45, A, ZrC, 43	Bottom edge	50	25	
9	WAR, 45, A, ZrC, 43	Severe at top	6	5	Re foil and BeO insulator attached
10	WAR, 45, A, SiC, 43	None	0	0	
11	WAR, 44, A, SiC, 40	None	0	0	
16	WAR, 45, A, SiC, 43	None	0	0	
17	WAR, 44, A, SiC, 48	Slight at top and bottom	0	0	
18	WAR, 44, A, SiC, 48		0	0	
19	WAR, 23, A, SiC, 44		0	0	
20	WAR, 45, A, SiC, 43		0	0	
21	WAR, 23, A, SiC, 44		0	0	

[a]WAR (denoting fuel particles obtained by pyrolysis of fuel-loaded weak-acid ion exchange resin) is followed by percent conversion = 100[1 — (1/2)(O/U)], resin type (A = Amberlite), SiC or ZrC coating in Triso design, and buffer thickness (μm).

was expected. As shown in Fig. 11, the rare earths are generally located with the uranium within the kernel. In Fig. 12, the ZrC doping of the oPyC layer can be seen in the Zr *La* display.

The fissile particles from rods 7 through 9 were recovered by electrolytic deconsolidation and examined with IMGA. The SiC-Triso particles from rods 16, 17, and 19 were located in an approximately equivalent position relative to the flux, in the bottom half of the capsule (Table 3). The IMGA histograms for these six rods show very poor performance for the fissile particles with ZrC coatings compared with the particles with SiC coatings (Figs. 13 and 14). The histograms of measured-to-calculated activity ratios of a volatile (^{137}Cs) to a stable (^{106}Ru) fission product suggest much better fission product retention by the particles with SiC-Triso coating designs (rods 16, 17, and 19). The measured activity ratios come from the IMGA analysis. The calculated ratios come

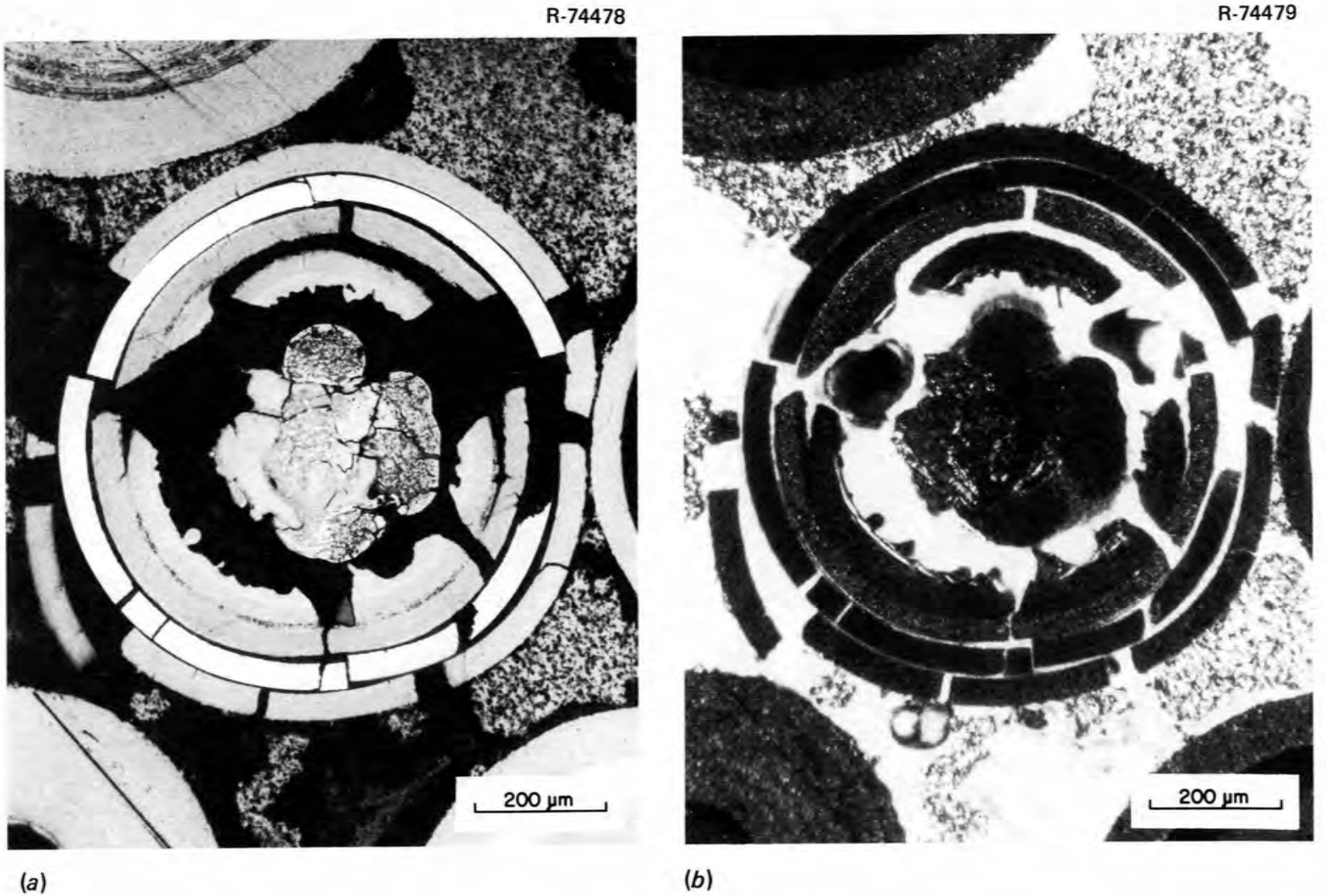

Fig. 7. Pressure-vessel failure of fissile particle from rod HRB-12-1. (*a*) Bright-field illumination. (*b*) Polarized-light illumination. This particle was located 1.1 mm from the outside of the fuel rod and operated at an average temperature of 990°C and an average temperature gradient of 450°C/cm. The hot side of the particle was on the right.

This Page Blank

This Page Blank

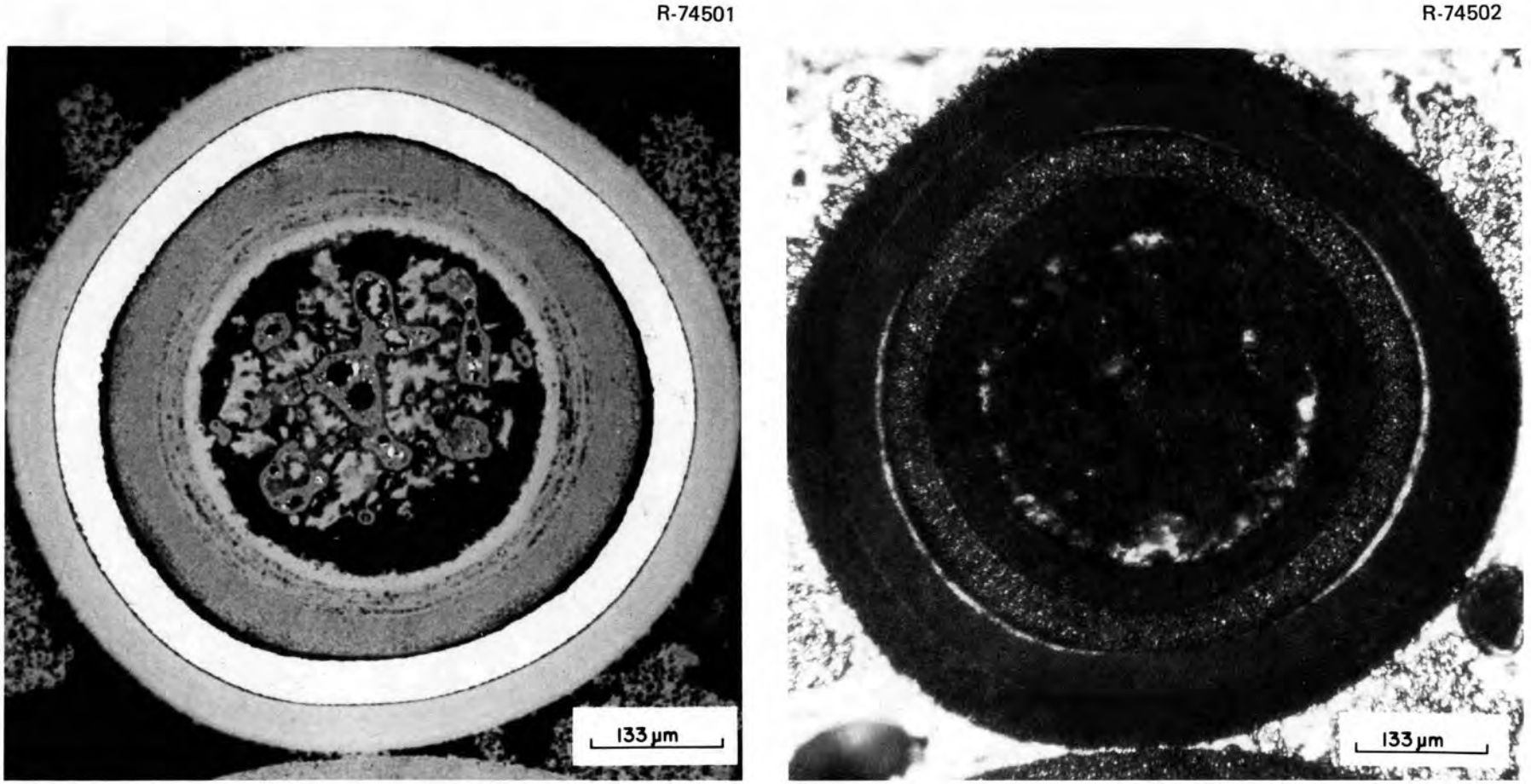

Fig. 10. Fissile particle from rod HRB-12-3. (*a*) Bright-field illumination. (*b*) Polarized-light illumination. This particle was 2.7 mm from the outside of the rod and operated with an average temperature of 1155°C and an average temperature gradient of 220°C/cm. The hot side of the particle was on the right.

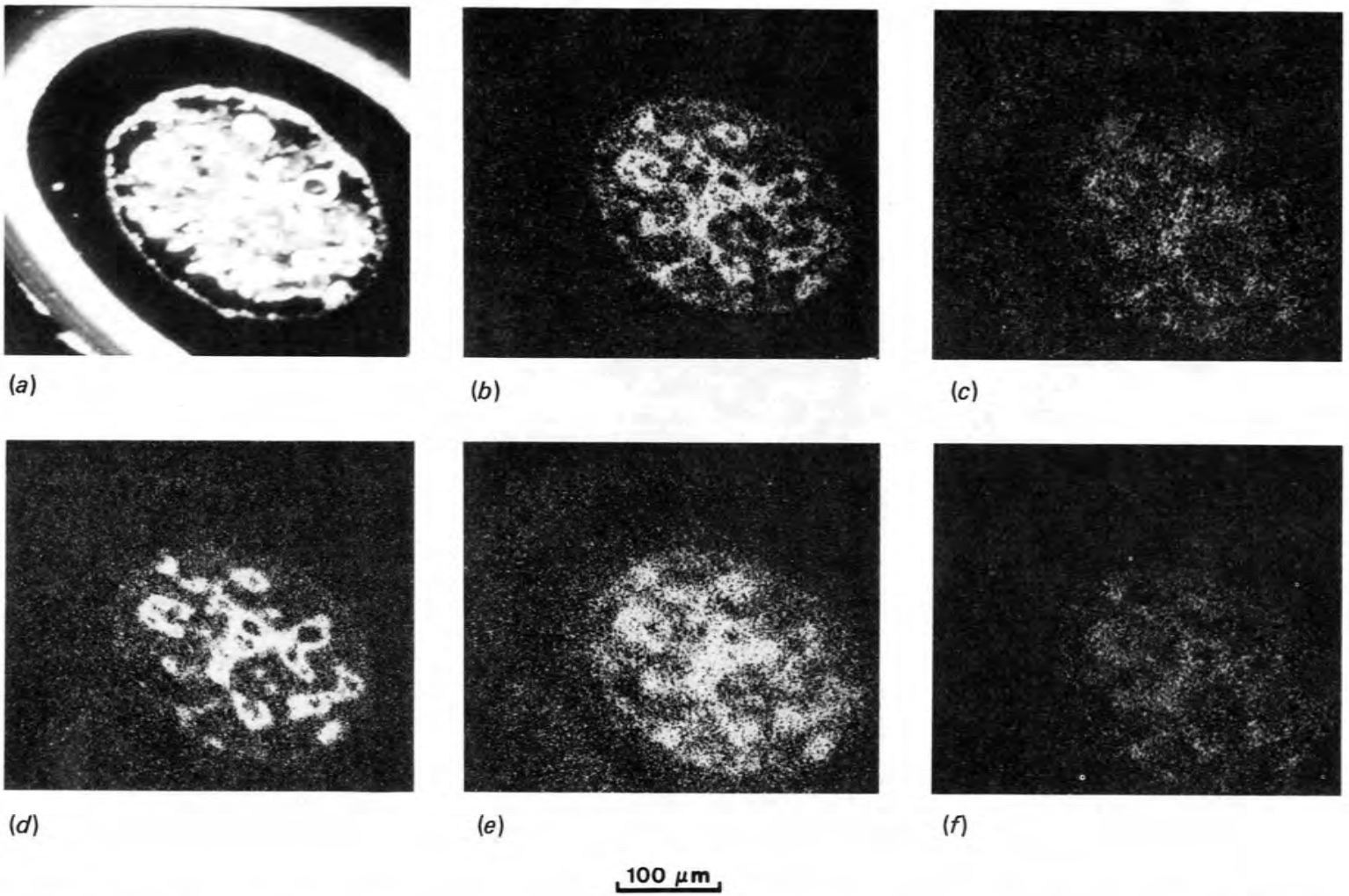

Fig. 11. X-ray displays from fissile particle from rod HRB-12-3 (same rod shown in Fig. 10). (*a*) Backscattered electron image. (*b*) Nd $L\alpha$. (*c*) Ce $L\alpha$. (*d*) U $M\beta$. (*e*) Pr $L\alpha$. (*f*) La $L\alpha$.

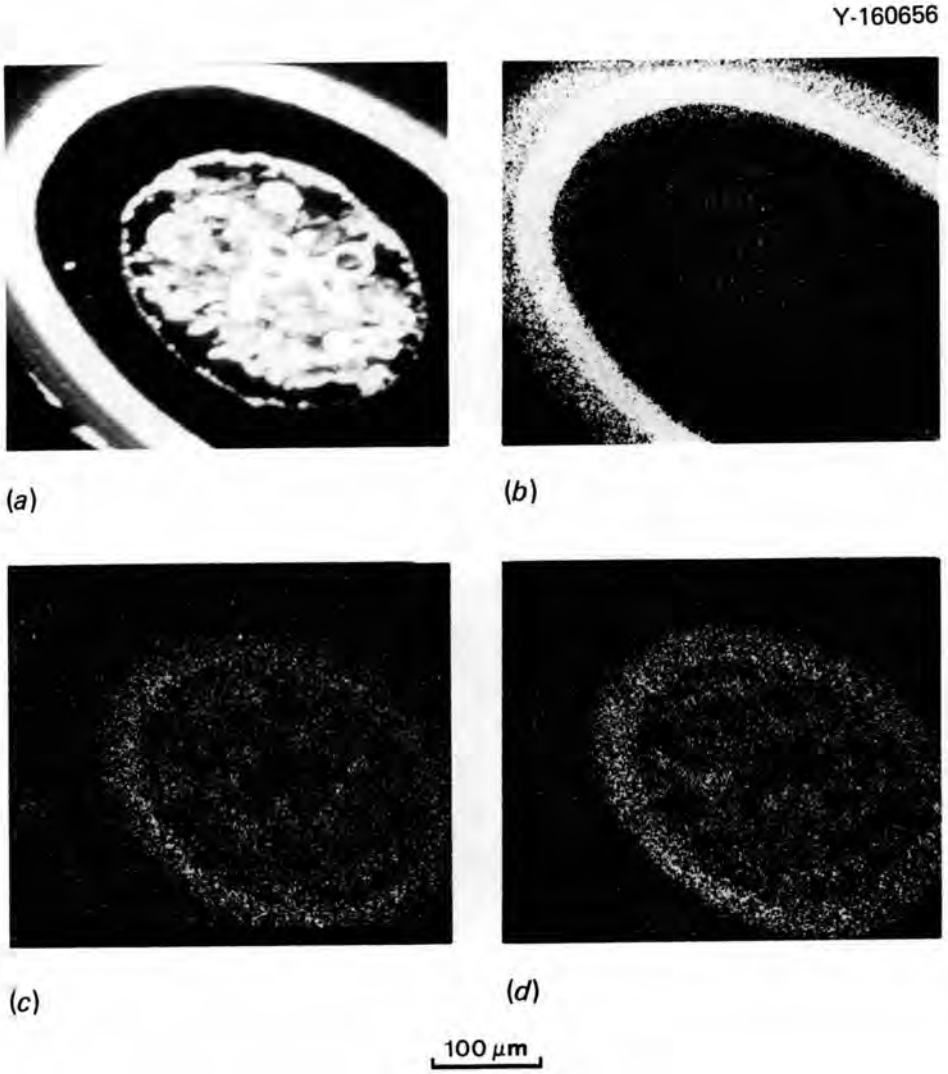

Fig. 12. X-ray displays from fissile particle from rod HRB-12-3 (same rod shown in Fig. 10). (*a*) Backscattered electron image. (*b*) Zr *Lα*. (*c*) Cs *Lα*. (*d*) Xe *Lα*.

from the burnup analysis. For particles with failed coatings we assume that the volatile cesium escapes, while the stable ruthenium remains within the kernel. Decisions relating to which of the particles shown in the histograms have actually lost cesium are based on analysis of the counting errors and calculational errors (Table 4).[13] For these batches the 90% confidence interval is about ±25% from the mean ratio. Therefore,

Table 3. Comparison of failure fractions for Triso-coated fissile particles with ZrC and SiC coatings (IMGA data)

Rod	Fast Fluence (neutrons/m^2) $E > 29$ fJ	Burnup (% FIMA) ^{235}U	Burnup (% FIMA) ^{238}U	Number of particles examined	Particles failed Number	Particles failed Percent	95% Confidence failure fraction range[a]
			ZrC coatings				
7	6.90×10^{25}	86	26.3	186	44	24	0.2 — 0.3
8	7.14	86	27.3	100	56	56	0.4 — 0.7
9	7.36	87	28.0	96	30	31	0.2 — 0.4
			SiC coatings				
16	7.34	87	27.7	171	18	11	0.07 — 0.2
17	7.14	86	26.8	92	1	1	0.01 — 0.07
19	6.85	86	24.6	172	14	8	0.06 — 0.15

[a]Based on binomial probability noted, M. J. Kania and H. Nickel, *Performance Assessment of the (Th,U)O_2 HT1 Biso Coated Particle Under PNP/HHT Irradiation Conditions*, JÜL-1785, Kernfurschungsanlaga Jülich, Jülich, Federal Republic of Germany, November 1980.

particles with measured-to-calculated activity ratios less than about 75% of the mean are categorized as having lost cesium. Two SiC-Triso batches in rods 16 and 19 had 11 and 8% failures, respectively (Table 3), and one SiC-Triso batch in rod 17 had 1% failures. A review of the fabrication data on each SiC-Triso batch did not indicate a definitive reason for the better performance in rod 17 than in other rods. The SiC-Triso batches performed well compared with the ZrC-Triso batches in rods 7, 8, and 9, which had failure rates of 24, 56, and 31%, respectively.

The poor performance of the fissile particles with ZrC coatings in capsule HRB-12 is described qualitatively in the gamma scan of the empty graphite sleeve (Fig. 15). The high activity in the energy range 0.55 to 0.75 MeV (which includes fission products ^{137}Cs, ^{154}Eu, ^{95}Zr, and ^{110m}Ag) at the top of the capsule (where the fissile particles with ZrC coatings were located) suggest high failure rates in the fuel rods located there during capsule operation. The HRB-12 scan can be compared with the HRB-11 scan (HRB-11 had no fissile particles with ZrC coatings), where the high activity was at the center (high burnup) portion of the sleeve (Fig. 16).

ORNL-DWG 83-15380

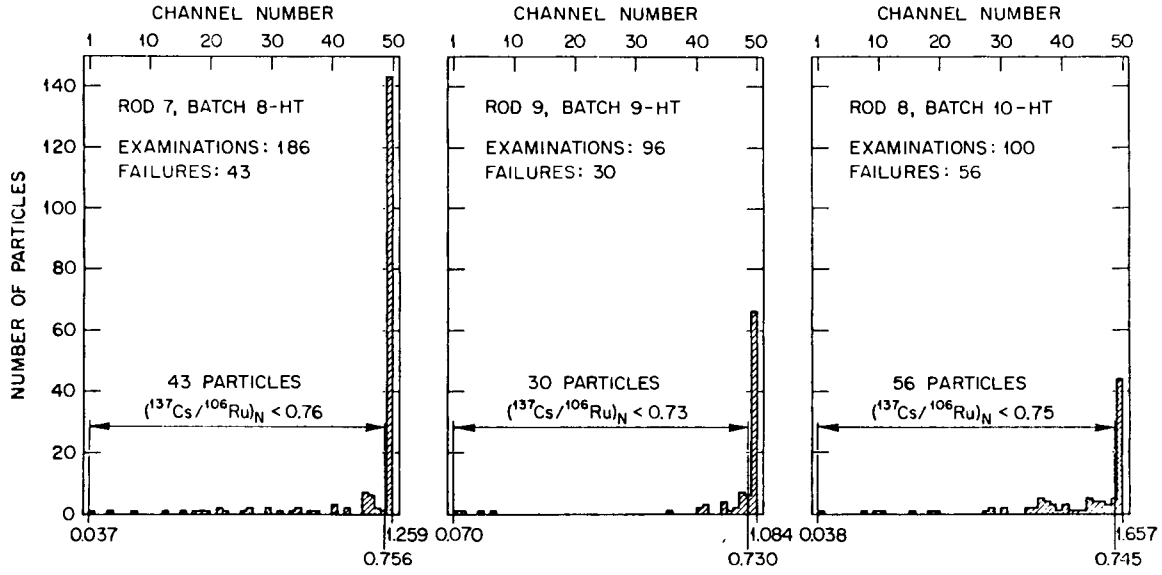

Fig. 13. Distribution of HRB-12-7, -8, and -9 particles with ZrC coatings according to ratio IMGA-measured $^{137}Cs/^{106}Ru$ to burnup-calculated $^{137}Cs/^{106}Ru$ (activity ratios).

ORNL-DWG 83-15560

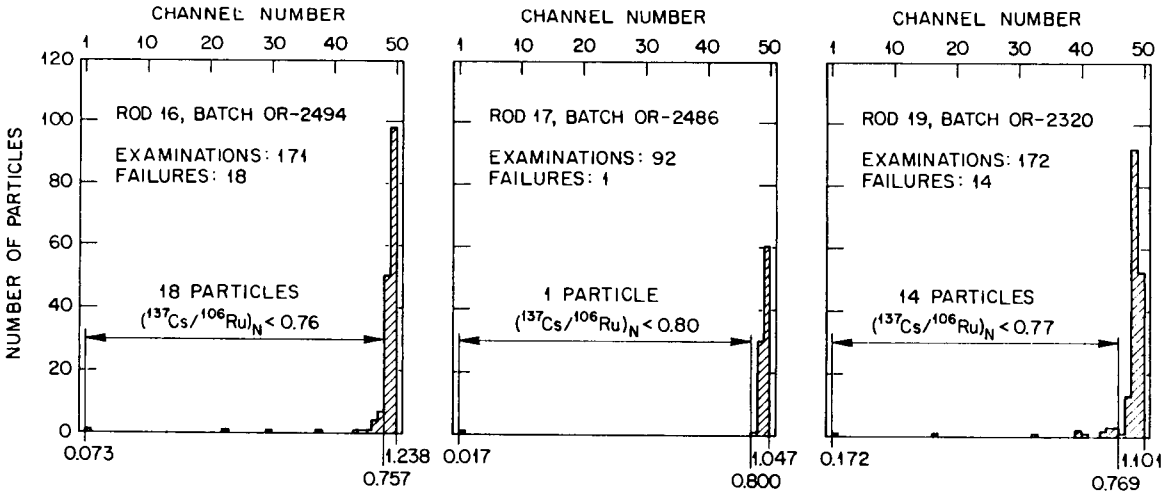

Fig. 14. Distribution of HRB-12-16, -17, and -19 particles with SiC coatings according to ratio IMGA-measured $^{137}Cs/^{106}Ru$ to burnup-calculated $^{137}Cs/^{106}Ru$ (activity ratios).

Table 4. Summary of errors in IMGA analysis of fission product retention by fissile particles from rods 7, 8, 9, 16, 17, and 19 irradiated in Capsule HRB-12

Fuel rod[a]	Counting errors (%)		Calculation errors (%)	Total errors (%)	90% Confidence interval (±1.645σ)
	^{106}Ru	^{137}Cs			
7(186)	5.6	0.74	15	16.0	26.4
8(100)	4.3	0.76	15	15.6	25.7
9(96)	<3.8	<0.7	15	15.5	25.4
16(171)	3.9	0.64	15	15.6	25.6
17(92)	3.6	0.69	15	15.5	26.4
19(172)	4.0	0.73	15	15.6	25.6

[a]Numbers enclosed by parentheses are the numbers of particles examined.

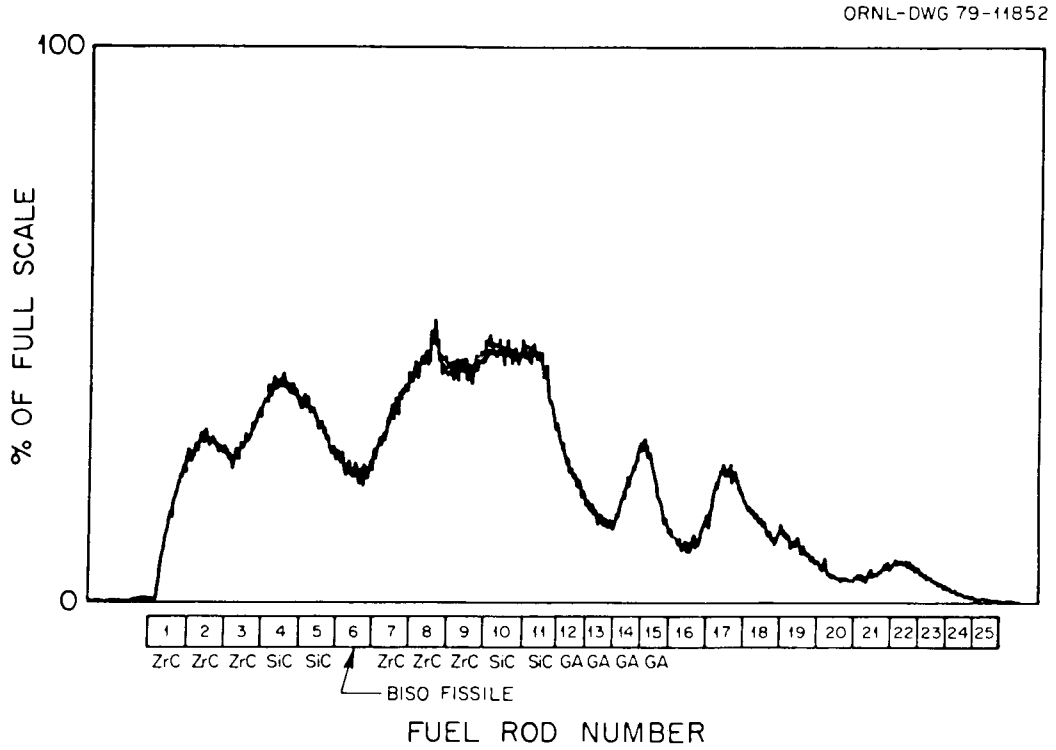

Fig. 15. Gross gamma scan of empty graphite sleeve from HRB-12. Full scale for this was 10^6 counts/min in the energy range 0.55 to 0.75 MeV. The lead collimator slit used was 3.2 mm wide. The highest activity release to the graphite sleeve appears to have come from the rods at the top of the capsule (left of figure), where the ZrC-coated fissile particles (fabricated by LANL) were located.

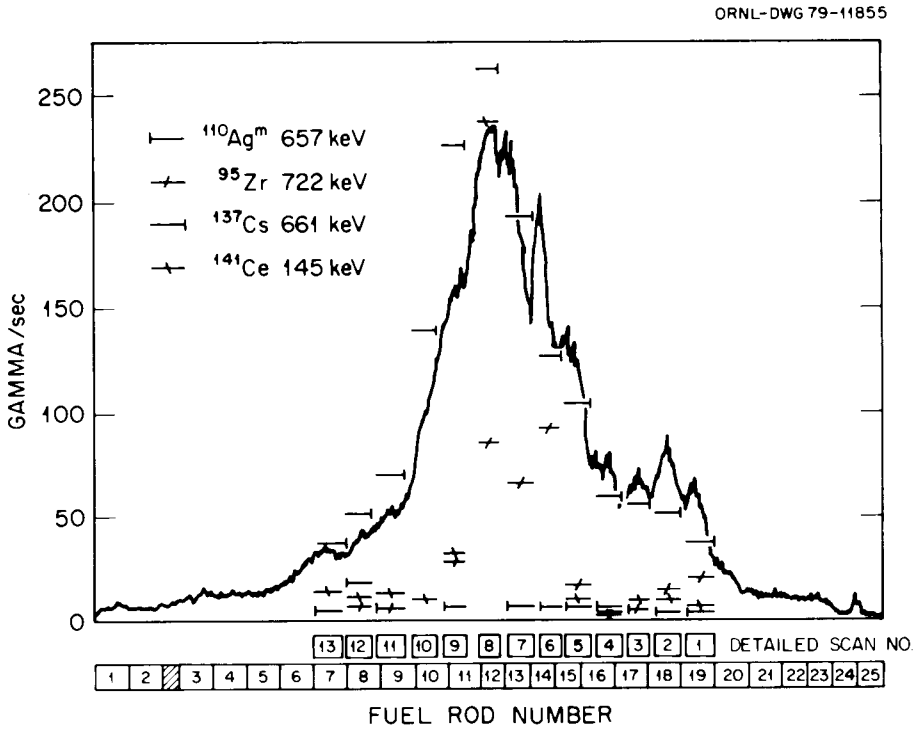

Fig. 16. Gross gamma scan of empty graphite sleeve from HRB-11. Full scale for this scan was 10^6 counts/min in the energy range 0.55 to 0.75 MeV. The lead collimator slit used was 3.2 mm wide. The highest activity release to the graphite sleeve appears to have come from the rods in the center of the capsule (probably 11 through 17). Activity data for specific fission products from Appendix B of F. J. Homan et al, *Irradiation Performance of HTGR Fuel Rods in HFIR Experiments HRB-11 and -12*, ORNL-5584, June 1980, are superimposed on the gross gamma scan (the *Y*-axis scale applied to these data). It appears that most of the activity in the sleeve comes from ^{137}Cs. Note that the 722-keV peak includes ^{154}Eu as well as ^{95}Zr.

CAPSULE HRB-15a

Capsule HRB-15a contained 18 fuel rods and 17 wafer-tray assemblies.[14] Fissile particles with the ZrC-Triso coating design were included in two of the fuel rods, one of the wafers, and three of the loose-particle trays. The ZrC-Triso fissile particles with both UO_2 and UC_2 kernels were tested. In addition to the ZrC-Triso fissile particles, two types of "buffered UO_2" kernels were tested with SiC-Triso coating designs. The UO_2^*(a) particle contained a ZrC-doped buffer layer, and the UO_2^*(b) particle contained a flash coating of dense PyC on top of the kernel, followed

by a thin layer (5 to 10 μm thick) of ZrC (in turn, followed by the iPyC, SiC, and oPyC layers). Particles with buffered UO_2 kernels were included in two fuel rods, four monolayers, and two loose particle trays.

Metallographic examination performed at GA on rod 6 revealed slight cracking of the ZrC coatings. This cracking was attributed to the metallographic preparation process rather than to irradiation damage, but because such cracking is rarely observed in SiC coatings, it was concluded that the ZrC coatings are more fragile than SiC. Some porosity was observed in the irradiated ZrC coatings from rod 6, and, because no porosity was observed in the as-fabricated condition, the porosity is concluded to be irradiation induced. No fission product attack of the ZrC coating was observed. A representative metallographic display is shown in Fig. 17.

Metallographic and microprobe studies performed on rod 7 at ORNL [ZrC-Triso with UC_2 kernel (Figs. 18 and 19)] show large accumulations of fission products in the iPyC layer.[15] This is shown in the polarized light views of Fig. 18. The high optical activity (bright areas in polarized light) indicative of the presence of fission products in the iPyC coating is characteristic of fuels with carbide kernels. The electron microprobe display (Fig. 19) shows cesium present in large concentrations in the buffer and iPyC layers. The rare earths (represented by La and Nd displays) are present at the iPyC-ZrC interface. Palladium is also present at this interface but does not seem to have attacked the ZrC. This indicates that ZrC is more resistant to fission product attack than SiC, because significant SiC attack was noted in SiC-Triso fissile particles irradiated in capsule HRB-15a.

The UO_2^*(b) fuel performed better than any of the other fissile particle types irradiated in Capsule HRB-15a. In many particles, the thin ZrC layer deposited over the kernel (the layer was expected to fail) did not fail. When the inner ZrC coating failed, the kernel extruded through the cracks into the buffer layer. This is not considered detrimental to particle performance. The presence of the thin ZrC coating effectively buffered the oxygen potential in the particles (which is the reason it was there), and no kernel migration was observed. Significant fission product

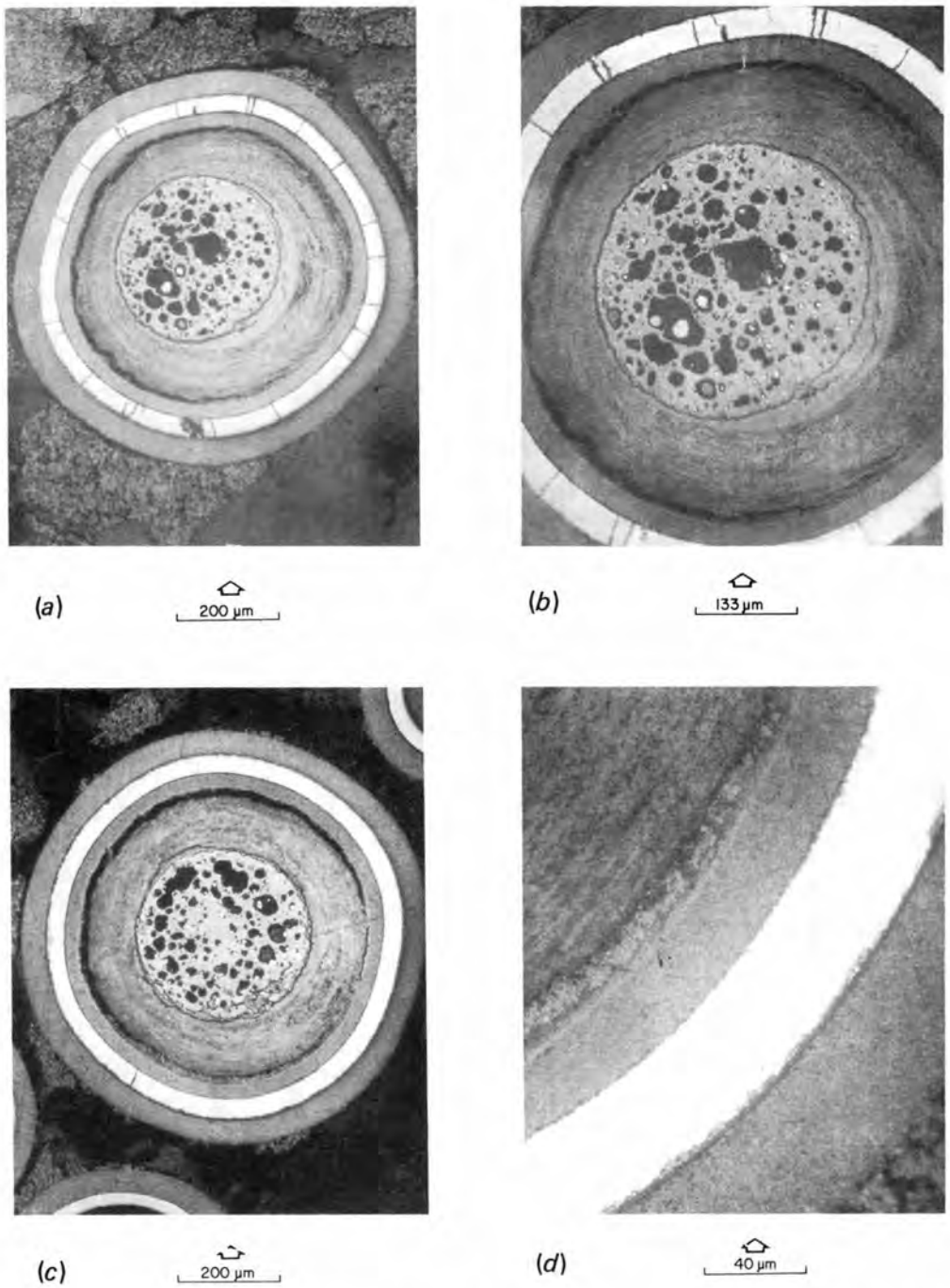

Fig. 17. Representative photomicrographs of fissile UO_2 ZrC-Triso particles (batch 6162-00-010) irradiated in fuel rod 6 to a fast neutron fluence of 6.2×10^{25} neutrons/m^2 ($E > 29$ fJ HTGR) and burnup 28.4% fissions per initial heavy metal atom (FIMA) at about 1200°C. (*a*) and (*c*) Typical particles. The ZrC cracks are due to polishing damage. (*b*) Kernel microstructure. (*d*) ZrC structure. The porosity in the ZrC was irradiation induced. Metallography courtesy of GA Technologies.

R-77411

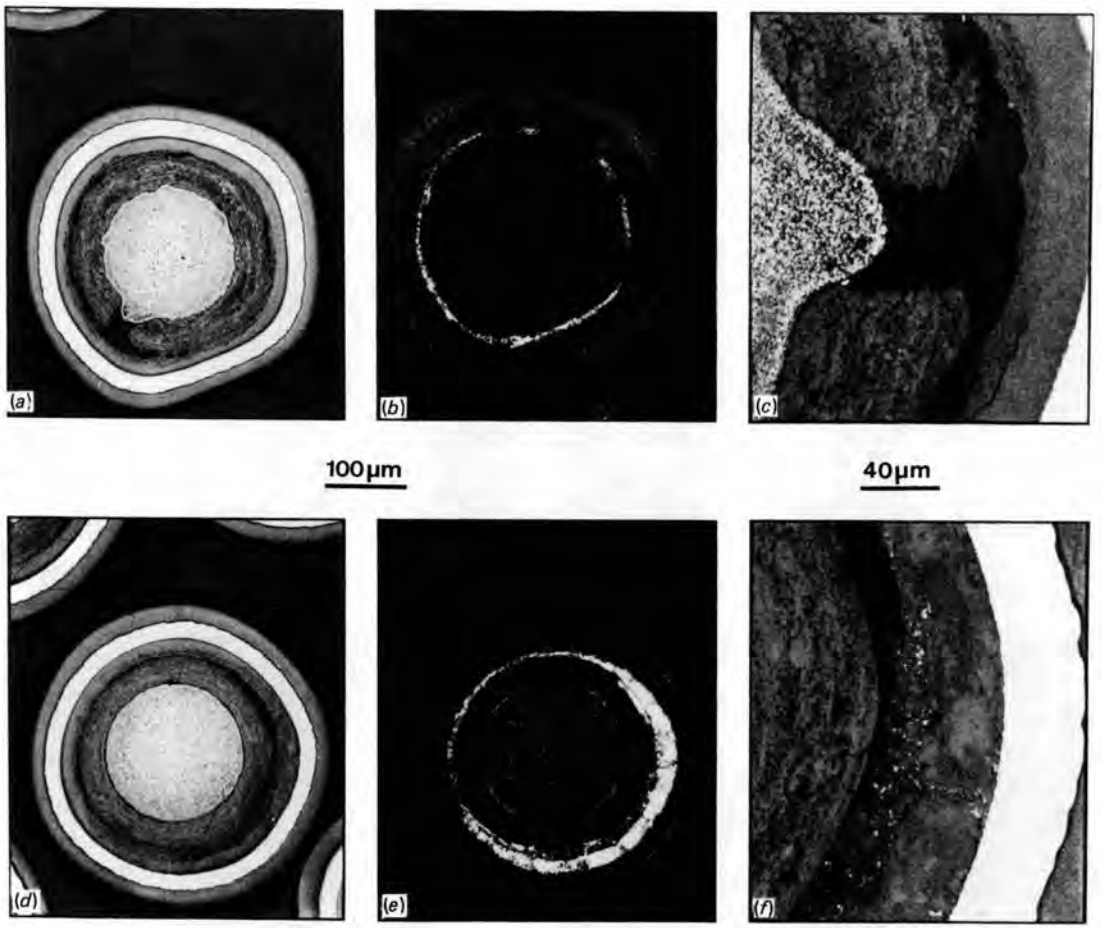

Fig. 18. Fissile particles from batch 6161-00-010, UC_2 kernel with a ZrC-Triso coating, irradiated in HRB-15a fuel rod 7. (*a*) and (*d*) Typical appearance of particles in bright-field illumination. (*b*) Polarized-light illumination of particle in (*a*). (*c*) Kernel-buffer interface of particle in (*a*). (*e*) Polarized-light illumination of particle in (*d*). (*f*) Fission product accumulation of inner PyC of particle in (*d*). Particles in rod 7 achieved a fast-neutron fluence of 6.6×10^{25} neutrons/m^2 ($E >$ 29 fJ) and a burnup of 28.3% fissions per initial heavy metal atom (FIMA) at 1191°C.

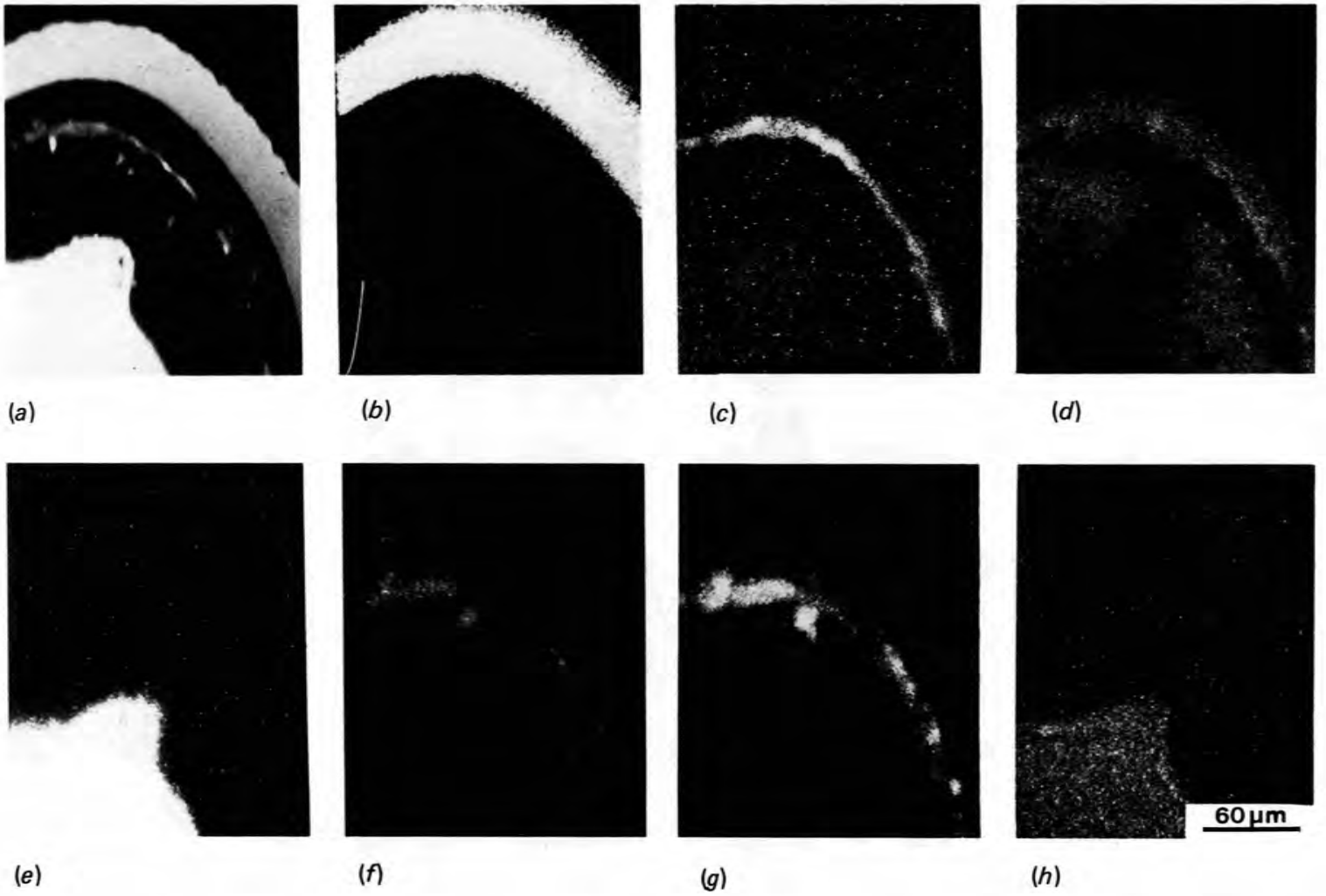

Fig. 19. X-ray displays of fissile particle, UC_2 kernel ZrC-Triso coated and irradiated in HRB-15a fuel rod 7. (*a*) Backscattered electron image. (*b*) Zr *Lα*. (*c*) Pd *Lα*. (*d*) Cs *Lα*. (*e*) U *Mβ*. (*f*)La *Lα*. (*g*) Nd *Lα*. (*h*) Mo *Lα*.

attack of the SiC coating was observed in some of these particles. Localized attack was observed in 64% of the particles examined metallographically, with penetration up to 50% of the way through the 35-μm SiC layers in some cases. Representative metallography from rod 9 is shown in Fig. 20.

Metallographic and microprobe studies performed on rod 2 at ORNL [UO_2^*(b)] show some interesting trends (Figs. 21 and 22). In Fig. 21(*a*), the thin ZrC layer deposited on top of the kernel was broken and some of the kernel material had moved into the cracks. The characteristic UO_2 appearance is evident, with gas bubbles throughout the kernel. In Fig. 21(*b*), the thin ZrC coating remained intact, and the kernel is considerably more dense. No gas bubbles are evident. About 30% of the particles observed metallographically from this rod had the appearance shown in Fig. 21(*a*). Figure 21(*c*) is a higher magnification of Fig. 21(*a*), and this same particle was examined with the electron microprobe (Fig. 22). The electron microprobe displays indicate that the rare earths were retained in the kernel (as expected for oxide fuels) and that cesium concentrated in the buffer and iPyC layers. Figure 23 (higher magnification) shows concentrations of palladium at the iPyC-SiC interface at points adjacent to where the ZrC layer was breached.

Visual examination of the loose-particle trays revealed no broken particles in trays 2, 5, 6, 12, or 15. These are the trays (see Table 1) that contained the ZrC-Triso particles with buffered UO_2 kernels. Details can be found in Ref. 15.

Postirradiation fission gas release-to-birth ratio (R/B) measurements made in the GA Triga reactor revealed the following failure rates for the rods with ZrC-Triso or buffered UO_2 fissile particles:

Rod	In-service failure (%)	Particle type
2	0	UO_2^*(b)
3	0.4	UO_2^*(a)
6	7.8	ZrC Triso (UO_2)
7	22.7	ZrC Triso (UC_2)
9	3.0	UO_2^*(b)
12	0.5	UO_2^*(b)

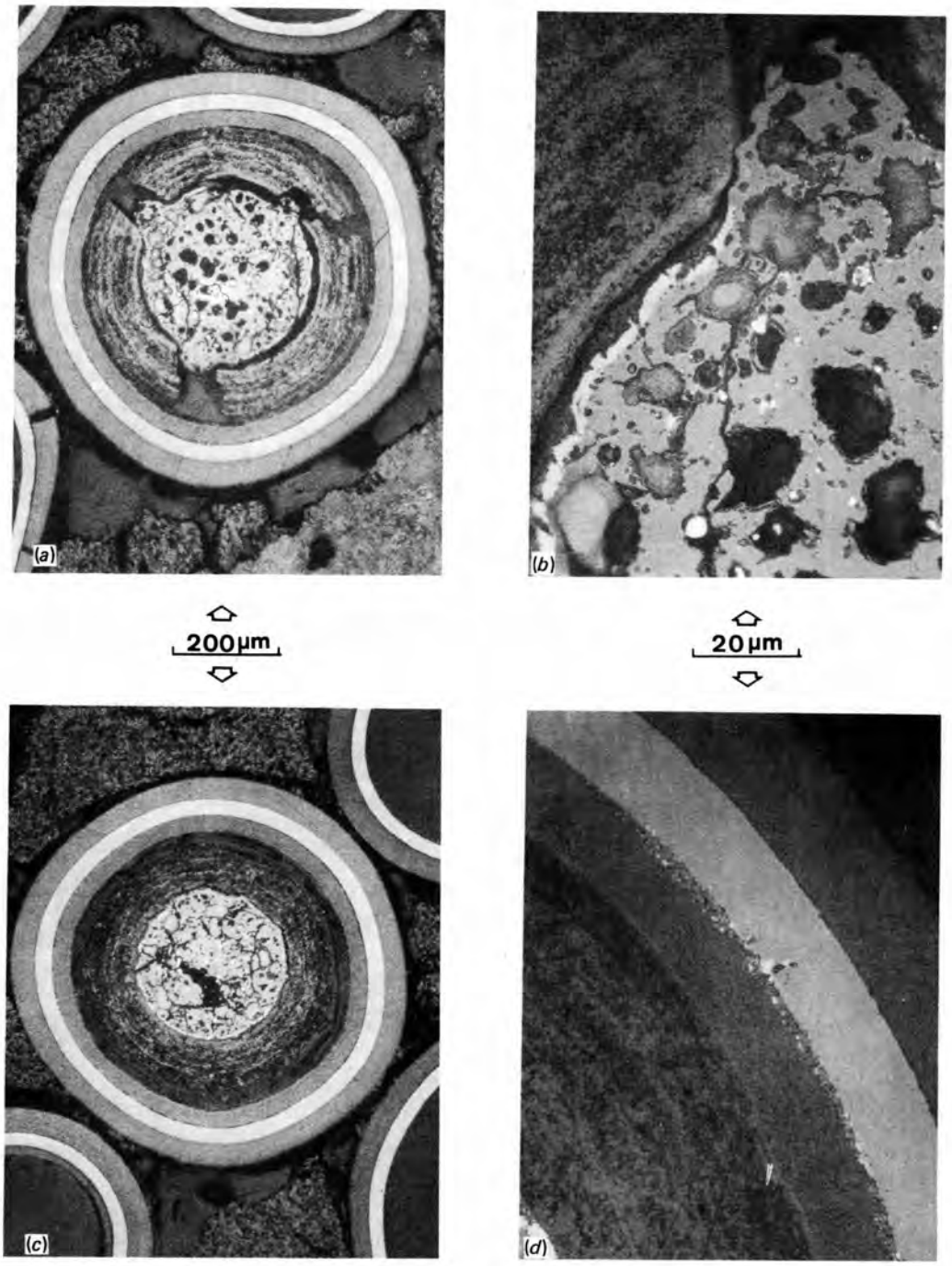

Fig. 20. Representative photomicrographs of fissile UO_2^*-Triso particles (batch 6152-06-010) irradiated in fuel rod 9 to a fast neutron fluence of 6.7×10^{25} neutrons/m^2 ($E > 29$ fJ HTGR) and burnup of 28.9% FIMA at about 1200°C. (*a*) and (*c*) Typical particles. (*b*) Example of kernel extrusion into a cracked buffer; note also the remainder of the ZrC placed on the kernel. (*d*) Example of severe SiC attack, that is, about 18 μm into SiC. Metallography courtesy of GA Technologies.

R-77410

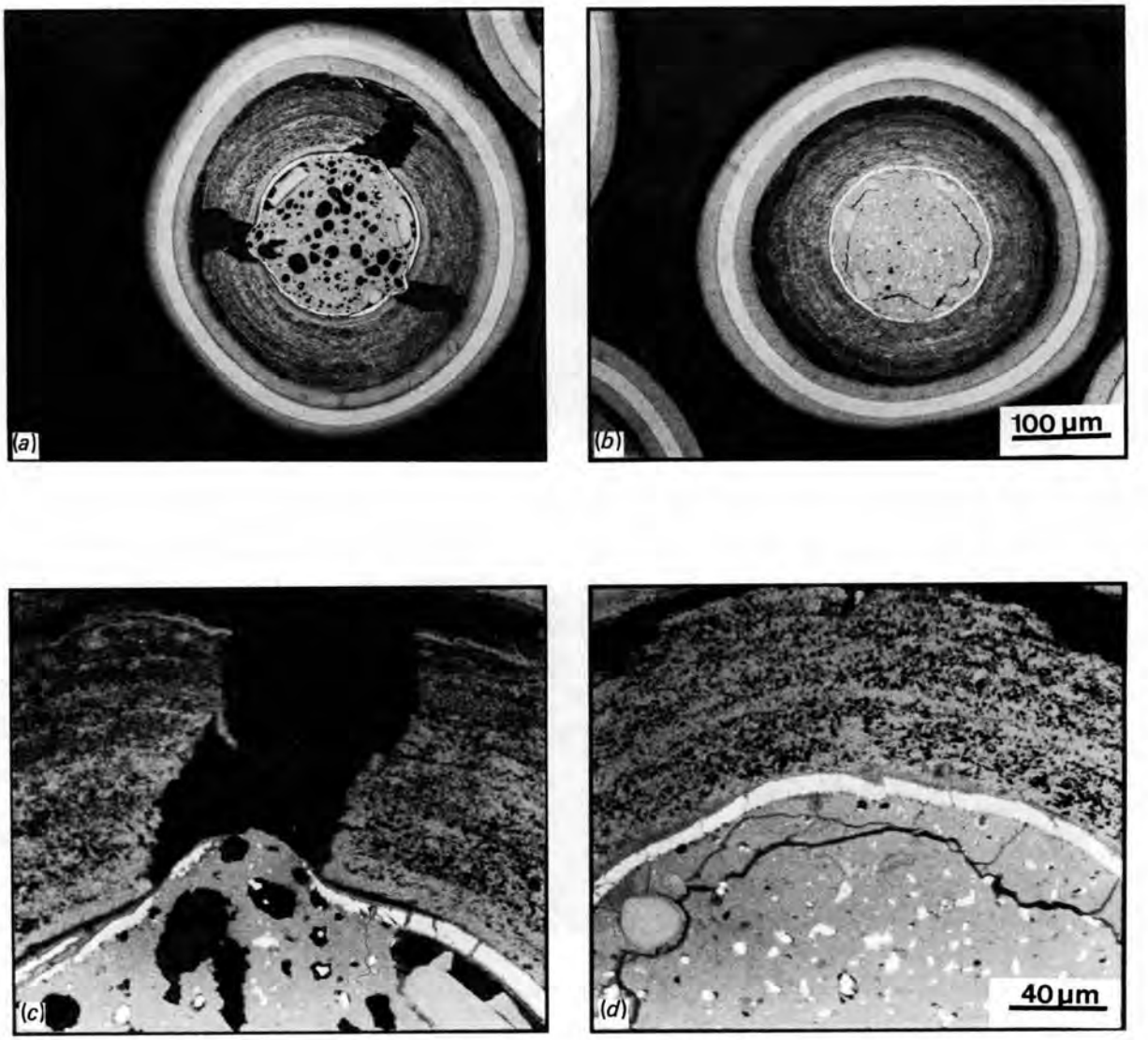

Fig. 21. Fissile particles from batch 6152-06-010, ZrC-buffered UO_2 kernel with a Triso coating, irradiated in HRB-15a fuel rod 2. (*a*) Typical appearance of particle with broken ZrC layer and cracked iPyC. (*b*) Typical appearance of particle with intact ZrC and coatings. (*c*) Kernel-buffer interface of particle from (*a*). (*d*) Kernel-buffer interface of particle shown in (*b*). Particles in rod 2 achieved a fast fluence of 4.6×10^{25} neutrons/m^2 ($E > 29$ fJ) and a burnup of 22.3% FIMA at 1103°C.

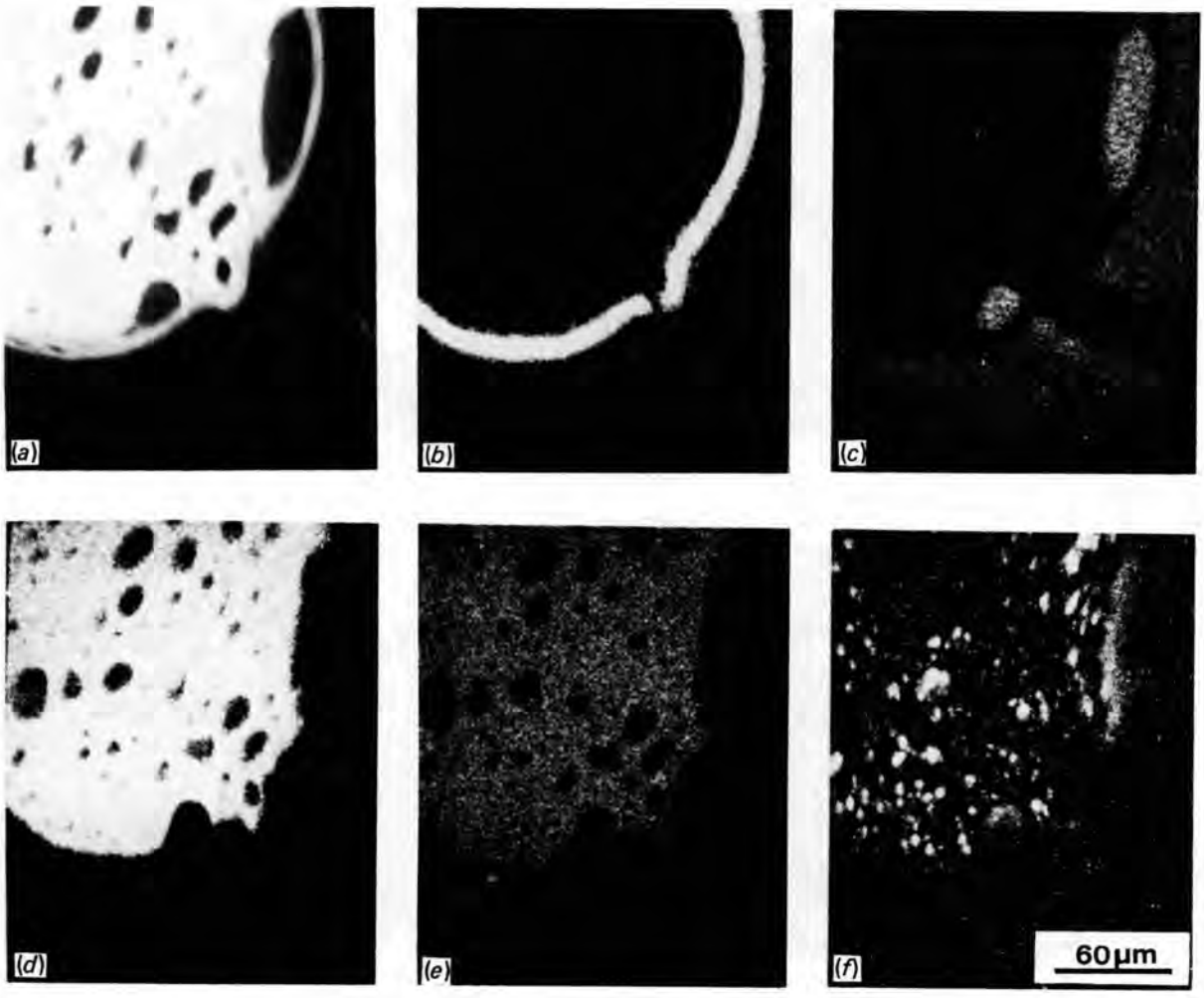

Fig. 22. X-ray displays of fissile particle, ZrC-buffered UO_2 kernel Triso coated, irradiated in HRB-15a fuel rod 2. (*a*) Backscattered electron image. (*b*) Zr *Lα*. (*c*) Cs *Lα*. (*d*) U *Mβ*. (*e*) Nd *Lα*. (*f*) Mo *Lα*.

The postirradiation R/B measurements on fuel rods include a contribution from both fissile and fertile particles; therefore, the measured ^{85m}Kr release cannot all be attributed to the fissile particles. However, the above data suggest that the ZrC-Triso fissile particles did not perform as well as the SiC-Triso particles with buffered UO_2 kernels.

The GA metallographic examination results on fissile particles irradiated in HRB-15a fuel rods are summarized in Table 5. Noteworthy from this table is that the ZrC-Triso particles are the only fissile particle type in which fission product attack of the primary pressure vessel layer was not observed.

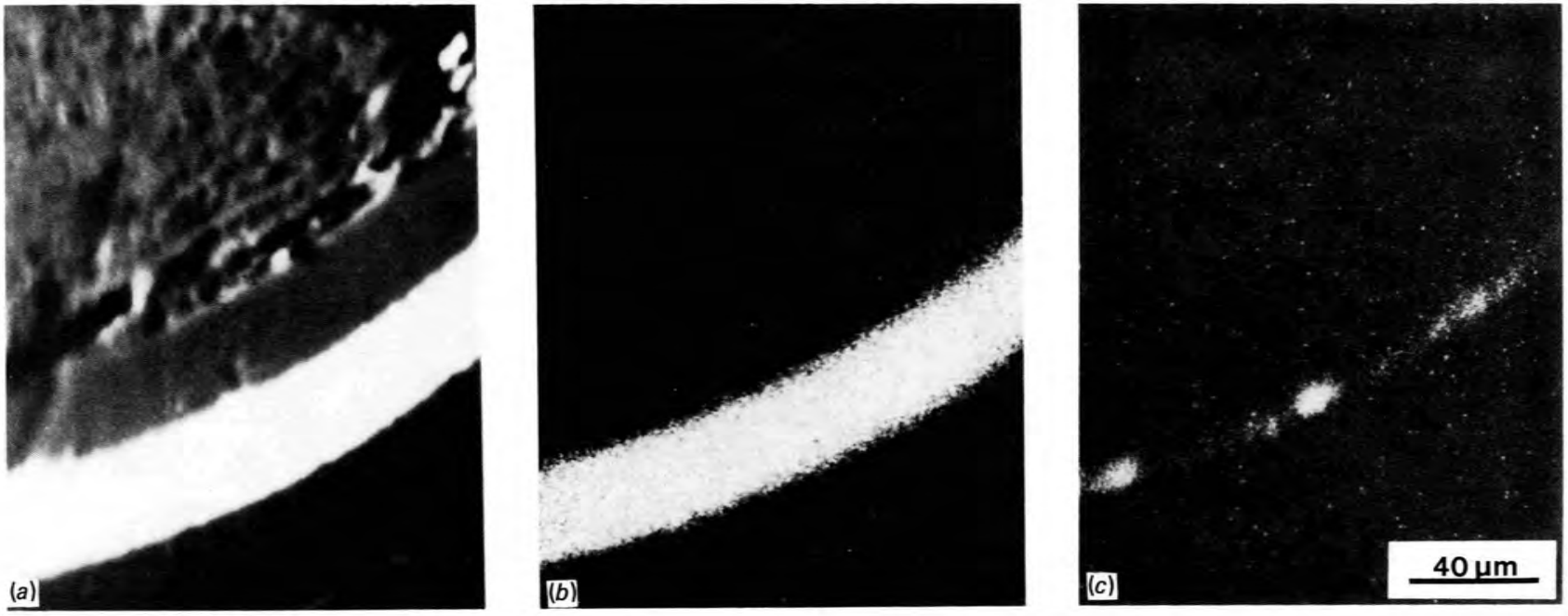

Fig. 23. X-ray displays of fissile particle, ZrC-buffered UO_2 kernel Triso coated, in Fig. 22 which was irradiated in HRB-15a fuel rod 2. (*a*) Backscattered electron image of iPyC-SiC interface. (*b*) Si $K\alpha$. (*c*) Pd $L\alpha$.

Table 5. Summary of HRB-15a fuel rod metallographic results from GA Technologies

Kernel type	Coating type	Particle batch	Fuel rod capsule position	Fast fluence (neutrons/m^2) (E > 29 fJ HTGR)	Burnup[a] (% FIMA)	Number of particles examined	Particles with kernel migration (%)	Cracked buffer (%)	Kernel extensions into buffer (%)	iPyC debonded (%)	iPyC failed (%)	iPyC coating reaction[b] (%)	SiC/ZrC coating reaction[c] (%)	SiC/ZrC tear (%)	SiC/ZrC+ oPyC failure (%)	Particles with porosity in ZrC (%)	oPyC failure (%)
$UC_{0.4}O_{1.6}$	Triso	6157-11-010	4	5.3×10^{25}	25.0	30	0	13.3	26.7	0	0	100	70.0	0	0		3.3
UO_2	ZrC-Triso[d]	6162-00-010	6	6.0	27.2	37	18.9	2.7	0	0	0	0	0	0	0	100	0
UO_2	Triso	6152-04-010	8	6.4	28.7	18	22.2	0	0	0	0	100	38.9	0	5.6		5.6
UO_2[e]	Triso	6152-06-010	9	6.5	29.0	22	0	13.6	27.3	4.5	4.5	100	63.6	0	0		0
UC_2	Triso	6151-23-020	11	6.3	29.0	32	0	40.6	43.8	21.9	0	100	50.0	0	0		0

[a]Calculated burnup values.

[b]Particles that exhibited large concentrations of metallic fission products in the iPyC layer.

[c]Particles that exhibited metallic fission product attack of the SiC layer; attack of <2 μm was not observable.

[d]ZrC replaces SiC in fissile particle batch 6162-00-010. All particles showed porosity in ZrC.

[e]ZrC layer on kernel.

Autoradiographic measurements made on unbonded particle trays from capsule HRB-15a are summarized in Table 6. Qualitative comparisons between particle types reveal no definite trends. The ZrC-Triso particles (trays 5, 6, and 15) generally show high levels of activity (indicating failed particles), but many of the SiC-Triso fissile particles show similar levels of activity.

Gamma scan data on the unbonded particle trays (without particles) are summarized in Table 7. The ZrC-Triso fissile particle type with UC_2 kernels appears to be the most releasing particle in the summary. Some of the Triso-coated fertile particles appear to have released more fission products than expected.

Gamma counting at GA on small numbers of unbonded particles (ten or fewer) is summarized in Table 8. All particles seem to have retained ^{137}Cs (except the SiBiso fertile particle). The ZrC-Triso fissile particle with UC_2 kernel lost most of its ^{154}Eu and ^{110m}Ag, but so did the SiC-Triso particles from tray 4.

Rods 1, 2, 7, 13, 15, and 17 from capsule HRB-15a were electrolytically deconsolidated at ORNL and examined with IMGA. Rod 7 contained ZrC-Triso particles with UC_2 kernels. With the electrolytical deconsolidation procedure the electrolyte solution is analyzed for uranium and thorium, to account for particles that have failed extensively and would not be counted with IMGA. Usually very little uranium and thorium are found in the electrolyte solution (less than the inventory of one particle). However, with the HRB-15a rods, significantly more uranium and thorium were found in the electrolyte solution than was expected (Table 9). Rod 7 contained the SiBiso fertile particles, which performed rather poorly in this experiment. The thorium content of nearly four particles was found in the electrolyte solution. The uranium content of nearly six fissile particles was found. How the thorium and uranium contents in the electrolyte should be considered relative to the failure fraction is not known. It is not known whether a small amount of uranium or thorium entered the electrolyte from many particles, or a lot from a few particles. We are treating the data as though it were a lot from a few particles, as though these particles were pressure vessel failures and not subsequently counted with IMGA.

Table 6. Capsule HRB-15a unbonded particle tray autoradiographic details

Unbonded fuel particle type			Tray Activities		Film[c] exposure (s)	Observations and comments
Kernel type	Coating type	Batch	β + γ contact (R/h)[a]	β only at 0.3 m (mR/h)[b]		
Depleted UC_2	Triso	6151-24-010	0.06	0.5	300	No concentrations of activity
UO_2^*(b)	Triso	6152-06-010	0.13	0.5	300	No concentrations of activity
UC_2	Triso	6151-23-010	12	1.0	20	One area of activity centered about a particle
$UC_{0.4}O_{1.6}$	Triso	6157-11-010	45	1.2	10	Large, active area covering the two inner rings of particles as if release was uniform and from those particles only
UC_2	ZrC-Triso	6161-00-010	30	5.0	7	Approximately half the particle holes were bright with activity, but locations were random over the tray
UO_2	ZrC-Triso	6162-00-010	1.3	1.0	30	Two areas of activity, neither of which is centered on particle locations
ThO_2	Triso	6252-21-101	*d*	1.0	*d*	Three active areas, two of which appear to be centered on particle locations; some correlation with oPyC failures
ThO_2	Triso	6252-24-010	*d*	800	*d*	Two bright areas on film; one centered on pressure vessel failed particle location, one at random
ThO_2	Triso	6252-25-020	*d*	0.4	*d*	Several distinct areas of activity; one correlates with an oPyC-failed particle, the rest do not
UC_2	Triso	6151-23-020	17	1.0	20	One large bright spot where particle failed by pressure vessel mode

Table 6. (continued)

Unbonded fuel particle type			Tray Activities		Film[c] exposure (s)	Observations and comments
Kernel type	Coating type	Batch	β + γ contact (R/h)[a]	β only at 0.3 m (mR/h)[b]		
UO_2	Triso	6152-04-010	0.40	0.5	300	One area of activity centered on a particle location
UO_2^*(b)	Triso	6152-06-010	0.36	0.5	300	Two areas of slight activity not at particle locations
ThO_2	Triso	6252-12COMP	3	0.5	30	No significant concentrations of activity
$UC_{0.4}O_{1.6}$	Triso	5157-11-020	12	0.5	20	Many areas of activity, some centered on particle locations as if release was not uniform over tray
UC_2	ZrC-Triso	6161-00-010	14[e]	4.0	4	Approximately half the particle locations have activity, and all are located on one side of the tray only
ThO_2	SiBiso	6542-43-010	25	0.5	15	One distinct area of activity located near inner ring of particles
UC_2	Triso	6151-23-020	15	0.5	20	One distinct activity area covering two particle locations on inner ring of tray

[a]Activity measured September 1981 at time autoradiographs were made.

[b]Activity measured November 1981 at time gamma scans were done.

[c]Film used was Industrex brand, type Sr-5; the exposure time had to be varied according to the activity level of the specimen.

[d]Not available.

[e]Measured 0.15 m (6 in.) from the tray.

Table 7. Gamma-scan data on HRB-15a unbonded particle trays (without particles) after irradiation

Tray	Unbonded fuel particle type			^{137}Cesium inventory			^{144}Cerium inventory			^{154}Europium inventory		
	Kernel type	Coating type	Batch	Measured[a] (μC)	Calculated[b] (μC)	(%[c] of inventory)	Measured[a] (μC)	Calculated[b] (μC)	(%[c] of inventory)	Measured[a] (μC)	Calculated[b] (μC)	(%[c] of inventory)
1	Depleted UC_2	Triso	6151-24-010	1.08 E0	2.03 E3	0.05		3.81 E4			2.26 E2	
2	UO_2^*(b)	Triso	6152-06-010	5.33 E0	8.77 E3	0.06		1.99 E5			5.50	
3	UC_2	Triso	6151-23-010	1.65 E1	8.66 E3	0.19		1.93 E5		1.41 E1	5.13 E2	2.75
4	$UC_{0.4}O_{1.6}$	Triso	6157-11-010	1.63 E1	7.42 E3	0.22		1.64 E5		5.51 E1	4.14 E2	0.13
5	UC_2	ZrC-Triso	6161-00-010	2.76 E1	8.51 E3	0.32	1.07 E4	1.86 E5	5.75	6.52 E1	4.50 E2	14.49
6	UO_2	ZrC-Triso	6162-00-010	3.38 E1	1.11 E4	0.31	1.08 E1	2.40 E5	<0.01	1.43 E0	5.60 E2	0.26
7	ThO_2	Triso	6252-21-010	3.22 E1	1.16 E4	0.28	1.43 E2	2.63 E5	0.05	2.70 E1	3.55 E2	7.61
8	ThO_2	Triso	6252-24-010	3.26 E1	1.20 E4	0.27	8.18 E1	2.73 E5	0.03	6.62 E-1	3.63 E2	0.18
9	ThO_2	Triso	6252-25-010	8.53 E0	1.13 E4	0.08	3.28 E0	2.58 E5	<0.01	1.85 E-1	3.42 E2	0.05
10	UC_2	Triso	6151-23-020	1.99 E0	8.16 E3	0.02	9.70 E2	1.75 E5	0.55	2.83 E0	3.88 E2	0.73
11	UO_2	Triso	6152-04-010	1.01 E0	9.45 E3	0.01	8.51 E0	2.03 E5	<0.01		4.57 E2	
12	UO_2	Triso	6152-06-010	1.75 E0	1.03 E4	0.02	1.10 E0	2.23 E5	<0.01		5.13 E2	
13	ThO_2	Triso	6252-12COMP	1.02 E0	4.95 E3	0.02	9.77 E0	1.13 E5	<0.01	2.17 E1	1.56 E2	13.91
14	$UC_{0.4}O_{1.6}$	Triso	6157-11-020	1.21 E0	7.05 E3	0.02	2.77 E0	1.55 E5	<0.01	1.29 E1	3.81 E2	3.39
15	UC_2	ZrC-Triso	6161-00-010	3.12 E0	8.10 E3	0.04	9.22 E3	1.79 E5	5.15	7.58 E1	4.62 E2	16.41
16	ThO_2	SiBiso	6542-43-010	6.76 E-1	4.87 E3	0.01		1.11 E5		2.80 E1	1.63 E2	17.18
17	UC_2	Triso	6151-23-020	7.66 E-1	7.02 E3	0.01		1.62 E5		8.48 E0	4.66 E2	1.82

[a]Gamma scan times were 15–30 min; inventories back-calculated to end of irradiation (Jan. 29, 1981); a geometry factor of 0.94 was applied to the measured data.

[b]Inventory in unbonded particles calculated with GA's CURIE code; calculated ^{154}Eu inventories were doubled.

[c](Measured inventory divided by calculated inventory) times 100.

Table 8. Retention of fission product nuclides in HRB-15a unbonded particles determined by gamma counting

Unbonded particle tray	Particle type		Particle batch	Number of particles scanned	Retention of nuclides[a] (%)							
	Kernel	Coating			^{137}Cs[b]		^{110m}Ag		^{154}Eu		^{144}Cr	
					Average	Range	Average	Range	Average	Range	Average	Range
4	$UC_{0.4}O_{1.6}$	Triso	6157-11-010	9	100	104–110	32	10–83	45	0–84	87	83–90
14	$UC_{0.4}O_{1.6}$	Triso	6157-11-020	10	100	105–109	57	10–82	78	0–102	88	83–91
3	UC_2	Triso	6151-23-010	5	100	104–108	84	80–90	84	67–103	100	98–103
10	UC_2	Triso	6151-23-020	5	100	107–111	78	72–81	100	99–119	99	90–107
17	UC_2	Triso	6151-23-020	5	100	108–111	73	67–83	61	23–81	97	91–103
12	UO_2(b)	Triso	6152-06-010	10	100	107–112	76	68–84	92	81–101	100	95–105
5	UC_2	ZrC-Triso	6161-00-010	10	100	102–106	37	13–56	46	0–75	88	82–97
6	UO_2	ZrC-Triso	6162-00-010	10	100	93–103	73	66–80	87	76–98	93	82–97
16	ThO_2	SiBiso	6542-43-010	10	97	95–99		c	50	0–95	95	92–97

[a]With ^{95}Zr as the immobile isotope.

[b]Values similar in ^{134}Cs.

[c]For this batch ^{110m}Ag statistics was poor (~20–30% 1σ).

Table 9. Equivalent numbers of failed fertile and fissile particle inventories based upon analytical results from HRB-15a fuel rod deconsolidation

Fuel rod	Fertile particle					Fissile particle				
	Batch	Number of particles per rod	Thorium content (mg)		Equivalent failed particles	Batch	Number particles per rod	Uranium content (mg)		Equivalent failed particles
			EOL[a]	Total recovered[b]				EOL[a]	Total recovered[c]	
1	6252-12 COMP	1654	0.38	0.48	1.3	6152-04-010	802	0.169	1.32	7.8
2	6252-12 COMP	1352	0.42	<0.08	<0	6152-06-010	650	0.160	1.24	7.8
7	6542-43-010	612	0.60	2.16	3.6	6161-00-010	377	0.170	0.96	5.9
13	6252-12 COMP	887	0.39	0.12	<0.3	6152-04-010	396	0.156	0.32	2.1
15	6542-43-010	668	0.58	0.36	<0.8	6151-23-010	423	0.157	0.60	3.8
17	6252-12 COMP	1340	0.41	0.08	<0	6157-11-020	717	0.168	0.52	3.1

[a]EOL = end-of-life heavy metal content of a single particle.

[b]Total thorium content recovered in the 400-mL electrolyte solution.

[c]Total uranium content applicable to fissile particles recovered in the 400-mL electrolyte solution.

The histograms of measured activity ratios for rods 7 and 15 are shown in Figs. 24 and 25. These histograms indicate that many of the fissile particles in rod 7 lost significant fractions of the ^{110m}Ag and ^{137}Cs inventories. The fissile particles in rod 15 were retentive by comparison. The measured and calculated activity ratios for all six rods examined from capsule HRB-15a are summarized in Table 10. On the average, the fissile particles tested in this capsule contained about 95% of the ^{137}Cs inventories and about half the ^{110m}Ag inventories (except for the particles in rod 17, which lost more than 80% of the ^{110m}Ag inventory). The Cs/Ru histograms were used to estimate failure fractions for these six rods, and that information is summarized in Table 11. This shows that the rod 7 fissile particles (ZrC-Triso) experienced the highest fraction of failures. This is consistent with the Triga data discussed earlier. The comparison between rods 7 and 15 is illustrated graphically by taking the measured activity ratios (Figs. 24 and 25) and dividing by the calculated activity ratios (Table 10) and replotting the histograms (Fig. 26).

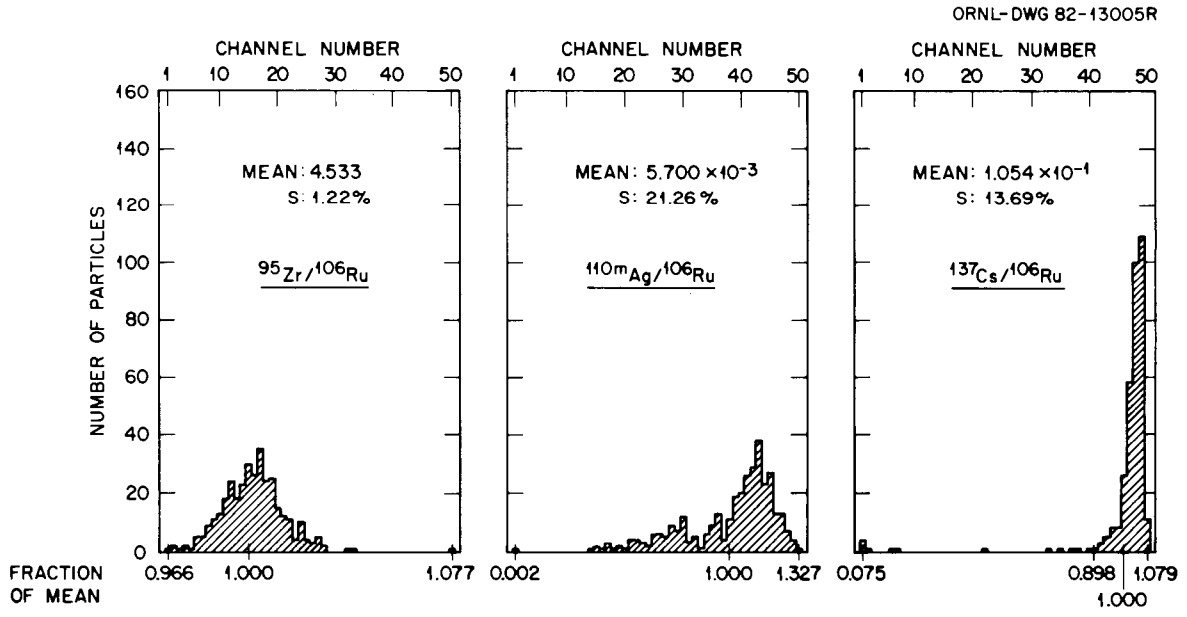

Fig. 24. An Irradiated Microsphere Gamma Analyzer (IMGA) analysis of particle batch 6161-00-010, a UC_2 kernel Triso-coated with ZrC, irradiated in fuel rod 7 of capsule HRB-15a (population size 342 particles).

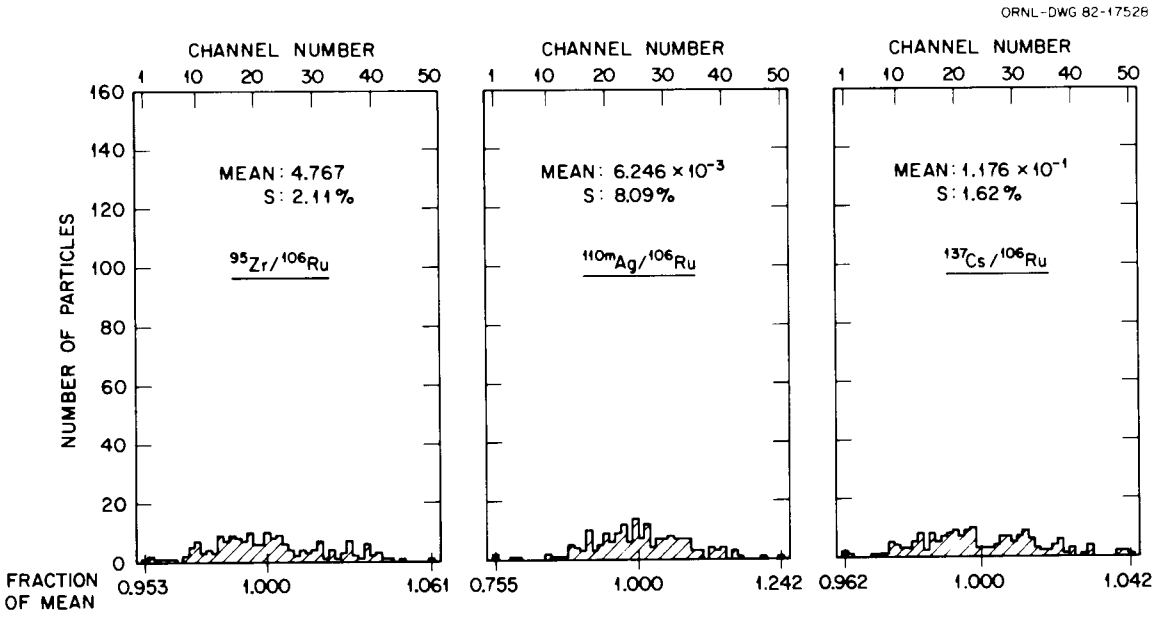

Fig. 25. An IMGA analysis of particle batch 6151-23-010, a UC_2 kernel Triso-coated, irradiated in fuel rod 15 of capsule HRB-15a (population size 184 particles).

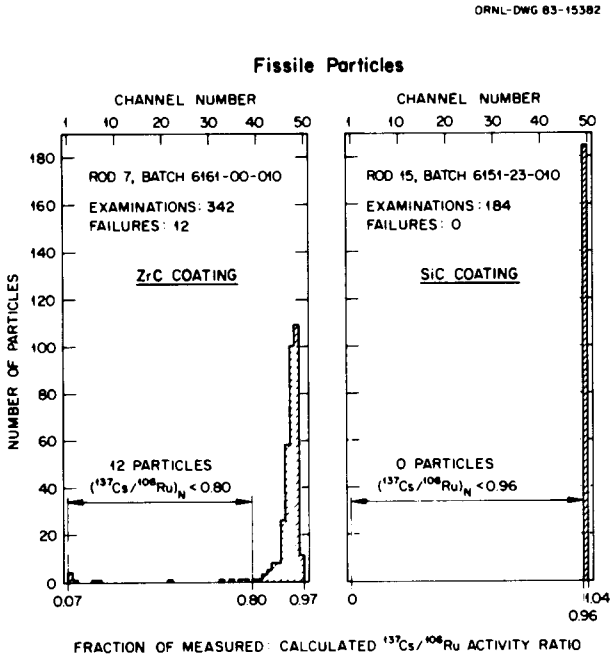

Fig. 26. Irradiation performance comparison for ZrC- versus SiC-Triso coatings based on $^{137}Cs/^{106}Ru$ activity ratios. The ZrC-coated particles were irradiated in position 7 and the SiC-coated particles in position 15 of capsule HRB-15a. The kernel material was UC_2 for both.

Table 10. Comparison between IMGA-derived activity ratios and calculated ratios for fissile particle batches irradiated in fuel rods 1, 2, 7, 13, 15, and 17 of capsule HRB-15a

Ratio	Gamma spectrometry data (IMGA)				Calculated ratio	Measured/Calculated	
	Minimum	Mean	Maximum	s(%)		Mean	Range
			Rod 1				
$^{95}Zr/^{106}Ru$	6.623	7.190	7.774	4.79	8.258	0.871	0.802–0.941
$^{110m}Ag/^{106}Ru$	2.261E-3	4.042E-3	5.737E-3	11.87	7.040E-3	0.574	0.321–0.815
$^{137}Cs/^{106}Ru$	1.446E-1	1.533E-1	1.612E-1	3.16	1.621E-1	0.946	0.892–0.995
$^{144}Ce/^{106}Ru$	3.020	3.223	3.440	3.38			
			Rod 2				
$^{95}Zr/^{106}Ru$	5.845	6.362	7.184	4.89	7.107	0.895	0.822–1.011
$^{110m}Ag/^{106}Ru$	3.468E-3	5.333E-3	7.302E-3	12.63	8.038E-3	0.663	0.431–0.908
$^{137}Cs/^{106}Ru$	1.020E-1	1.421E-1	1.554E-1	3.30	1.460E-1	0.973	0.699–1.064
$^{144}Ce/^{106}Ru$	2.608	2.786	3.141	3.21			
			Rod 7				
$^{95}Zr/^{106}Ru$	4.378	4.533	4.882	1.22	4.999	0.907	0.876–0.977
$^{110m}Ag/^{106}Ru$	9.955E-6	5.700E-3	7.562E-3	21.26	1.037E-2	0.550	0.001–0.730
$^{137}Cs/^{106}Ru$	7.909E-3	1.054E-1	1.137E-1	13.69	1.127E-2	0.935	0.070–1.008
$^{144}Ce/^{106}Ru$							
			Rod 13				
$^{95}Zr/^{106}Ru$	4.048	4.238	4.433	1.81	4.976	0.852	0.813–0.891
$^{110m}Ag/^{106}Ru$	1.122E-3	5.266E-3	7.878E-3	31.77	1.039E-2	0.507	0.108–0.758
$^{137}Cs/^{106}Ru$	8.890E-2	1.086E-1	1.129E-1	1.95	1.122E-1	0.968	0.792–1.006
$^{144}Ce/^{106}Ru$	2.106	2.192	2.289	1.62			
			Rod 15				
$^{95}Zr/^{106}Ru$	4.544	4.767	5.056	2.11	5.352	0.891	0.849–0.945
$^{110m}Ag/^{106}Ru$	4.716E-3	6.246E-3	7.759E-3	8.09	9.932E-3	0.629	0.475–0.781
$^{137}Cs/^{106}Ru$	1.132E-1	1.176E-1	1.225E-1	1.62	1.919E-1	0.987	0.950–1.028
$^{144}Ce/^{106}Ru$	2.160	2.571	2.788	4.93			
			Rod 17				
$^{95}Zr/^{106}Ru$	5.457	5.860	6.326	3.25	6.868	0.853	0.795–0.921
$^{110m}Ag/^{106}Ru$	9.637E-4	1.375E-3	6.301E-3	125.66	8.289E-3	0.166	0.000–0.760
$^{137}Cs/^{106}Ru$	3.748E-2	1.406E-1	1.500E-1	6.57	1.369E-1	1.027	0.174–1.095
$^{144}Ce/^{106}Ru$	2.637	2.878	3.114	3.87			

DISCUSSION AND CONCLUSIONS

The performance potential envisioned for ZrC-coated particles has not yet been demonstrated in the limited irradiation testing conducted to date. Although ZrC-coated particles have not performed as well as companion Triso-coated particles, the ZrC fabrication technology has received a small fraction of the attention devoted to SiC. As the focus of the

Table 11. Failed particle fractions from IMGA measurements

Rod	TRIGA measured failed particle fraction[a]	IMGA Examination			
		Number of fissile particles examined	Number failed	Failure fraction	95% confidence internal for failure fraction
1	0	467	0	0	<0.0065
2	0	365	1	0.0027	0.0005—0.02
7	0.231	342	12	0.035[b]	0.02—0.05[b]
13	0.002	201	1	0.005	0.001—0.03
15	0.028	184	0	0	<0.018
17	0.0002	345	4	0.012	0.005—0.03

[a]Fissile and fertile. Data from J. W. Ketterer et al., *Capsule HRB-15A Postirradiation Examination Report*, GA-A16758, GA Technologies, Inc., San Diego, in publication.

[b]The most conservative way to treat the electrolyte data (Table 9) is to add the number of particles corresponding to the uranium or thorium inventories measured in the electrolyte solution directly to the number of failures determined by IMGA. For the fissile particles counted with IMGA this operation makes a difference only for rod 7, where the measured failure fraction goes from 0.035 to 0.047, and the 95% confidence interval goes from 0.02—0.05 to 0.02—0.07. More likely, the uranium in the electrolyte solution comes from particles that are later counted with IMGA and identified as failed (and therefore counted in the failed particle fraction).

HTGR fuel development effort has narrowed to qualification of the low-enriched uranium (LEU)-Th reference fuel, funds available to continue the development of ZrC technology have dwindled to zero. The logic behind selection of the LEU-Th reference fuel was that this system would perform satisfactorily for any chosen HTGR application. However, the application of primary interest at the time of the selection was steam cycle cogeneration, the lowest temperature technology. If in the future a higher technology application (such as process heat) is favored, ZrC coatings may be considered again. The performance of SiC coatings is known to degrade with increasing temperature, and additional development of ZrC may produce a coating with superior performance in the regime of interest for the process heat reactor.

It is interesting to note that the UO_2^* particles irradiated in capsule HRB-15a performed better than any of the other candidate LEU-Th fissile fuel particles tested in that experiment. These particles were designed with a thin ZrC coating applied over the kernel (after a dense PyC flash coating was deposited) to prevent thermal migration of the UO_2 kernel. Although the thin ZrC coating was expected to fail early in the irradiation, in many cases it did not. The ZrC coatings tested in capsule HRB-15a probably represent the "state of the art" at the time ZrC coating technology was discontinued. These coatings performed very well and provide a strong point of departure should interest in the ZrC coating concept reemerge in the future.

ACKNOWLEDGMENTS

The authors would like to acknowledge the efforts of several people who contributed to the content of this report. We would like to acknowledge P. Wagner of the Los Alamos National Laboratory for his expertise and help in the area of ZrC coating deposition and for providing most of the coated particles used in this evaluation. We acknowledge E. L. Long, Jr., and T. N. Tiegs for their evaluation of the metallographic examinations; L. G. Shrader, who performed the metallography; and T. J. Henson, who performed the electron microprobe examinations. We also acknowledge G. A. Moore of the Operations Division, who performed the gamma spectrometry. We also thank D. P. Stinton and T. B. Lindemer for their technical review of this report. The authors acknowledge those who assisted in the preparation of this report: Sigfred Peterson for technical editing and Teresa Miller for composition and makeup.

REFERENCES

1. G. H. Reynolds et al., "Irradiation Behavior of Experimental Fuel Particles Containing Chemically Vapor Deposited Zirconium Carbide Coatings," *J. Nucl. Mater.* **62**, 9–16 (1976).

2. P. Wagner et al., "ZrC, a Key Ingredient for High Temperature Nuclear Fuels," *Symposium on Gas Cooled Reactors with Emphasis on Advanced Systems*, Jülich, Federal Republic of Germany, October 1975 (IAEA-SM-200/18).

3. C. M. Hollabaugh et al., "A New Method for Coating Microspheres with Zirconium Carbide-Carbon Graded Coats," *J. Nucl. Mater.* 57, 325–32 (1975).

4. C. M. Hollabaugh et al., "Chemical Vapor Deposition of Zirconium Carbide Alloyed Isotropic Carbon in a Fluidized Bed," pp. 419–29 in *Proceedings of the 6th International Conference on Chemical Vapor Deposition*, Atlanta, October 1977.

5. P. Wagner et al., "Factors Influencing the Chemical Vapor Deposition of ZrC," *J. Nucl. Mater.* 62, 221–28 (1976).

6. C. M. Hollabaugh et al., "Chemical Vapor Deposition of ZrC Made by Reactions of $ZrCl_4$ with CH_4 and with C_3H_6," *Nucl. Technol.* 35, 527–35 (1977).

7. R. D. Reiswig et al., *Behavior of LASL-Made Graphite, ZrC, and ZrC-Containing Coated Particles in Irradiation Tests HT-28 and -29*, LA-6211, Los Alamos National Laboratory, Los Alamos, N. Mex., May 1976.

8. T. N. Tiegs et al., *Irradiation Performance of HTGR Fuel in HFIR Capsule HT-31*, ORNL-5510, May 1979.

9. P. Wagner et al., *Irradiation Test HT-31: High-Temperature Irradiation Behavior of LASL-Made Extruded Fuel Rods and LASL-Made Coated Particles*, LA-6785-MS, Los Alamos National Laboratory, Los Alamos, N. Mex., April 1977.

10. E. L. Long, Jr., et al., *Performance of HTGR Fertile Particles Irradiated in HFIR Capsule HT-32*, ORNL/TM-7035, April 1980.

11. P. Wagner et al., *Irradiation Test OF-2: High Temperature Irradiation Behavior of LASL-Made Fuel Rods and LASL-Made Coated Particles*, LA-6988-MS, Los Alamos National Laboratory, Los Alamos, N. Mex., October 1977.

12. T. N. Tiegs and K. R. Thoms, *Operation and Postirradiation Examination of ORR Capsule OF-2: Accelerated Testing of HTGR Fuel*, ORNL-5428, March 1979.

13. M. J. Kania and K. H. Valentine, *The Irradiated-Microsphere Gamma Analyzer (IMGA) - An Integrated System for HTGR Coated Particle Fuel Performance Assessment*, ORNL-5606, February 1980.

14. J. W. Ketterer, "Preirradiation Description of GA Fuel in Capsule HRB-15a," unpublished GA Technologies data, September 1982.

15. J. W. Ketterer et al., *Capsule HRB-15A Postirradiation Examination Report*, GA-A16758, GA Technologies Inc., San Diego, July 1984.

ORNL/TM-9085
Distribution
Category UC-77

INTERNAL DISTRIBUTION

1–2. Central Research Library
3. Document Reference Section
4–5. Laboratory Records Department
6. Laboratory Records, ORNL RC
7. ORNL Patent Section
8. A. J. Caputo
9. W. P. Eatherly
10–14. F. J. Homan
15–19. M. J. Kania
20–29. P. R. Kasten
30. W. J. Lackey
31. F. R. Mynatt
32. A. R. Olsen
33. P. L. Rittenhouse
34. J. P. Sanders, Sr.
35. J. L. Scott
36. R. L. Senn
37. C. O. Slater
38. J. O. Stiegler
39. O. K. Tallent
40–42. P. T. Thornton
43. C. D. West
44. J. H. Wilson
45. R. J. Charles (Consultant)
46. H. F. Cook (Consultant)
47. Alan Lawley (Consultant)
48. T. B. Massalski (Consultant)
49. J. C. Williams (Consultant)
50. K. M. Zwilsky (Consultant)

EXTERNAL DISTRIBUTION

50–51. DOE, Division of High Temperature Reactor Development, Office of Converter Reactor Deployment, Washington, DC 20545

J. E. Fox
R. Ng

52. DOE, Office of Converter Reactor Deployment, Washington, DC 20545

Director

53. DOE, San Francisco Operations Office, 1333 Broadway, Oakland, CA 94612

L. Lanni

54. DOE, Oak Ridge Operations Office, P.O. Box E, Oak Ridge, TN 37831

Office of Assistant Manager for Research and Development
Attention: P. J. Gross/M. Rohr

55–173. DOE, Technical Information Center, P. O. Box 62, Oak Ridge, TN 37831

For distribution as shown in DOE/TIC-4500, Distribution Category UC-77 (Gas-Cooled Reactor Technology)